

Synthesis of Triptycene-Based Molecular Rotors for Langmuir–Blodgett Monolayers

Jiří Kaleta,^{*,†} Eva Kaletová,[†] Ivana Císařová,[§] Simon J. Teat,^{||} and Josef Michl^{†,‡}

[†]Institute of Organic Chemistry and Biochemistry, Academy of Sciences of the Czech Republic, Flemingovo nám. 2, 16610 Prague, Czech Republic

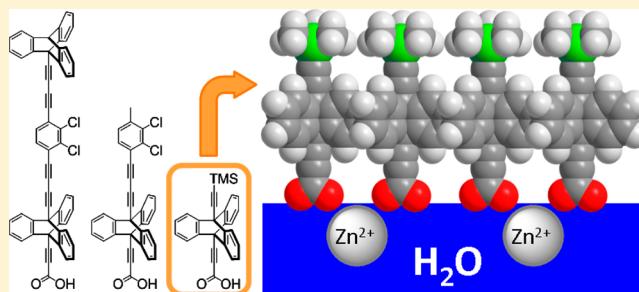
[§]Department of Inorganic Chemistry, Faculty of Science, Charles University in Prague, Hlavova 2030, 12840 Prague 2, Czech Republic

^{||}Advanced Light Source, Lawrence Berkeley National Laboratory, 1 Cyclotron Road, Berkeley, California 94720, United States

[‡]Department of Chemistry and Biochemistry, University of Colorado, Boulder, Colorado 80309-0215, United States

Supporting Information

ABSTRACT: We describe syntheses of six triptycene-containing molecular rotors with several single-crystal X-ray diffraction analyses. These rod-shaped molecules carrying an axial rotator are designed to interleave on an aqueous surface into Langmuir–Blodgett (LB) monolayers containing a two-dimensional trigonal array of dipoles rotatable about an axis normal to the surface. Monolayer formation was verified with the simplest of the rotor structures. On an aqueous subphase containing divalent cations (Mg^{2+} , Ca^{2+} , Zn^{2+} , Sr^{2+} , or Cd^{2+}), the LB isotherm yielded an area of $53 \pm 3 \text{ \AA}^2/\text{molecule}$ (monolayer of type A), compatible with the anticipated triangular packing of axes normal to the surface. On pure water, the area is $30 \pm 3 \text{ \AA}^2/\text{molecule}$, and it is proposed that in this monolayer (type B), the molecular axes are tilted by $40\text{--}45^\circ$ to a structure similar to those observed in single crystals of related triptycenes. After transfer to a gold surface, ellipsometry and PM IRRAS yield tilt angles of $29 \pm 4^\circ$ (monolayers of type A) and $38 \pm 4^\circ$ (type B). A full-scale examination of monolayers from all the rotors on a subphase and after transfer is underway and will be reported separately.



INTRODUCTION

The development of molecular rotors, in which one part of the molecule (the rotator) can turn relative to the rest (the stator), has been intensively pursued as documented by recent reviews, book chapters, and articles.^{1–14} In a search for collective dielectric behavior, especially of the ferroelectric type, we are particularly interested in preparing regular arrays of azimuthal dipolar rotors mounted on a surface. An extended and defect-free trigonal planar arrangement of dipoles is expected to favor a ferroelectric ground state.¹⁵ To achieve the desired order, we are relying on supramolecular chemistry, which allows extensive self-correction of possible defects. Up to now, we took advantage of guest–host interactions between molecular rotors and the walls of trigonally spaced hollow channels in the flat surface of a crystalline host matrix, hexagonal TPP [tris(*o*-phenylenedioxy)cyclotriphosphazene],^{7–9,16,17} and this effort is continuing.

Presently, we introduce a different approach to supramolecular assembly of trigonal two-dimensional arrays of azimuthal dipolar rotors, using the Langmuir–Blodgett (LB) monolayer technique.¹⁸ As a first step, we describe the synthesis of a new generation of amphiphilic molecular rotors for use in the preparation of LB monolayers of molecular rotors. There is

precedent for ferroelectric LB monolayers^{19,20} and multilayers²¹ and for other types of ultrathin ferroelectric films,^{22–24} but to our knowledge, regular LB arrays of dipolar molecular rotors have not been prepared before.

It is already known that triptycenes^{25,26} and similarly shaped structures²⁷ tend to pack on a surface in a way that produces the trigonal or hexagonal planar patterns shown in Figure 1. We decided to take advantage of this tendency and designed a new type of amphiphilic triptycene-based rods for LB applications (Chart 1).

The molecular rotors described below contain four essential structural motifs:

- An anchoring group that forces the terminal bond to orient perpendicular to the surface of an aqueous subphase. Carboxylic acid was chosen in the present study.
- A Y-shaped unit whose aromatic rings organize and stabilize the monolayer by intermolecular π – π interaction among neighbors. The length of the paddles

Received: July 29, 2015

Published: September 18, 2015

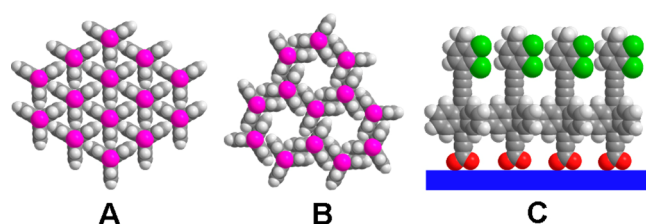
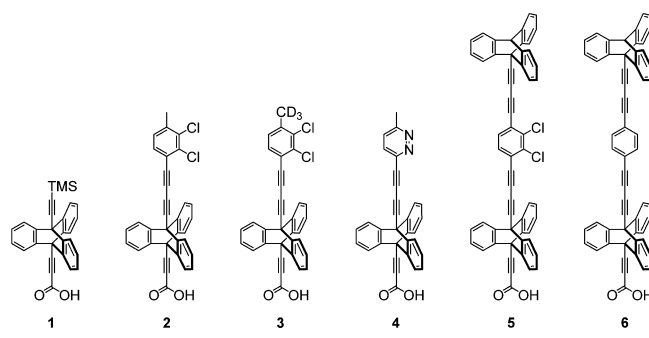


Figure 1. (A) Trigonal and (B) hexagonal arrangement of rotors (purple balls represent rotators installed on triptycene molecules). (C) Idealized model of a LB film formed from a single layer of molecular rotors 2 on aqueous subphase (side view).

Chart 1. Structures of Molecular Rotors 1–6



defines the distance between rotators. Triptycene was chosen to keep the distance short.

- (iii) An axle that provides sufficient separation between the triptycene and the dipolar rotator, in order to guarantee its nearly free rotation. A triple bond represents the simplest such unit, and a 1,3-butadiyne axle was chosen to provide sufficient length.
- (iv) A dipolar rotator, which is the functional heart of the dipolar molecular rotor. It must have a significant transverse dipole moment, but must be much less hydrophilic than the carboxyl group in order to ensure a proper orientation of the molecular rotor on the subphase. Its diameter must be smaller than the array lattice constant (the distance between neighboring rotors) to prevent their mechanical interactions (gearing effect). It is economical for the dipole to be generated by atoms other than oxygen, since they can then simultaneously serve as internal standards in XPS analysis of the monolayers after transfer to a solid substrate. As in our work on rotors inserted into TPP,^{9,14} we chose the 2,3-dichlorophenyl and 3-pyridazinyl groups. The dipole moment of *o*-dichlorobenzene is 2.5 D²⁸ and that of pyridazine is 4.1 D.²⁹

The molecular rotor 1 was prepared as a simple model structure for investigating the LB assembly on a trough. The CD₃ group in 3 is meant to serve as an IR chromophore with

well-defined transition moment directions that will help to measure the orientation of rotor axes relative to the plane of the monolayer. The price to pay for the length of the butadiyne axle is increased flexibility, which could permit sufficient bending to allow neighboring rotors to aggregate and perturb the regularity of the trigonal lattice. In an effort to preempt this potential problem, we have incorporated a triptycene unit on each side of the rotator in 5 and 6 and expect them to assemble into a more rigid “double-decker” monolayer structure, in which the rotators are located between two identical triptycene scaffolds. The rotor 6 with a nonpolar rotator was synthesized to provide baseline reference in future structural and dielectric studies.

RESULTS

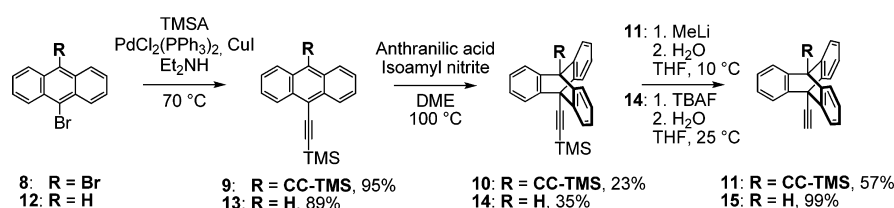
We describe the synthesis of 1–6, provide an X-ray structure analysis of nine triptycene derivatives, examine the formation of LB monolayers from the model compound 1 on various aqueous subphases, and characterize them by ellipsometry, contact angle, and polarization modulation infrared reflection–absorption spectra (PM-IRRAS). The preparation and thorough characterization of LB monolayers from the new rotor molecules 2–6 will be described separately.

Synthesis. The syntheses of all six molecular rotors follow a straightforward scenario, in which the construction of the triptycene core is followed by installation of a rotator and finally, in the last step, of the anchoring carboxylic group, whose presence reduces the solubility of the final product.

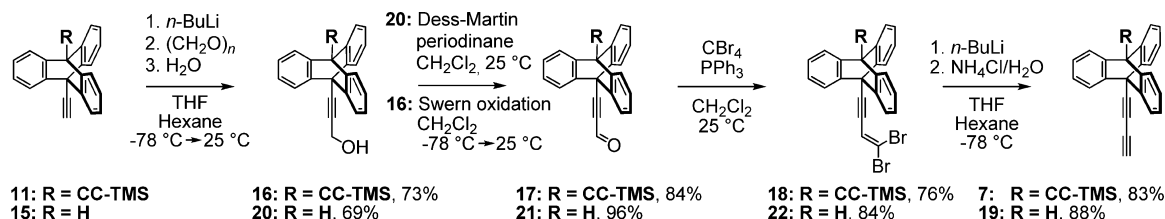
The key intermediate 7 was made from 9,10-dibromoanthracene (8) in seven steps. Coupling of 8 with trimethylsilylacetylene provided the silylated derivative 9 in an almost quantitative yield.³⁰ Subsequent Diels–Alder addition of benzyne, generated *in situ* from anthranilic acid and isoamyl nitrite in refluxing dimethoxyethane, resulted in the silylated triptycene 10 in an acceptable yield on multigram scale.^{14,31} Statistical desymmetrization of 10 using MeLi in THF at 10 °C afforded the alkyne 11 in a 57% isolated yield (Scheme 1).²⁸ Starting with commercially available 9-bromoanthracene (12), analogous steps produced the silyl derivative 13,³² the triptycene 14,³³ and the alkyne 15.³⁰

Stepwise construction of an additional triple bond on the singly protected triptycene 11 followed a protocol previously published for the symmetric 9,10-diethynyltriptycene.¹⁴ Selective lithiation of 11 with *n*-BuLi at –78 °C followed by reaction with paraformaldehyde yielded the alcohol 16, whose Swern oxidation gave the ynone 17 in 84% yield. Reaction with CBr₄ in the presence of PPh₃ resulted in the dibromo derivative 18. *n*-BuLi induced dehydrobromination of 18 at –78 °C provided the terminal alkyne 7 in a 83% yield (Scheme 2). The alkyne 15 was converted into the diyne 19 in a similar fashion. The formation of the alcohol 20, its oxidation to the aldehyde 21,³⁴ conversion to the dibromo derivative 22, and subsequent

Scheme 1. Preparation of Triptycene Derivatives 11 and 15

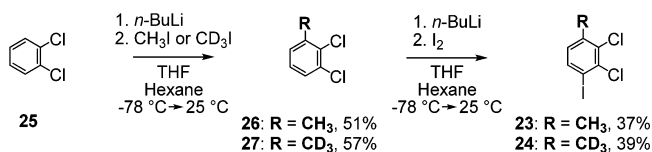


Scheme 2. Synthesis of Alkynes 7 and 19



dehydrobromination to **19** proceeded in similar yields as the reactions of their TMS analogues. All reactions with *n*-BuLi required a low temperature to prevent unwanted TMS cleavage.

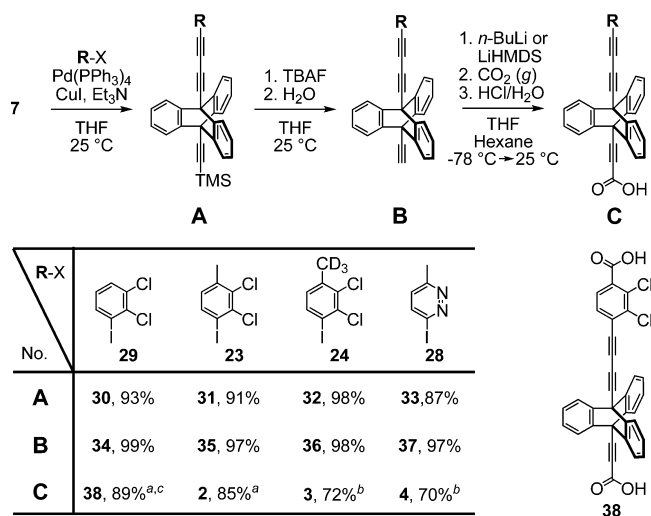
The halogenated toluenes **23** and **24** were synthesized in two steps from 1,2-dichlorobenzene (**25**), taking advantage of the acidity of its ortho hydrogen atoms. Selective deprotonation of **25** was performed using a slight excess of *n*-BuLi at $-78\text{ }^{\circ}\text{C}$. Low temperature suppressed undesirable elimination. Subsequent addition of CH_3I or CD_3I afforded corresponding toluenes **26** and **27**. A second deprotonation of **26** and **27** followed by reaction with I_2 provided the iodo derivatives **23** and **24** in $\sim 40\%$ yield (Scheme 3).

Scheme 3. Two-Step Preparation of **23** and **24** from **25**

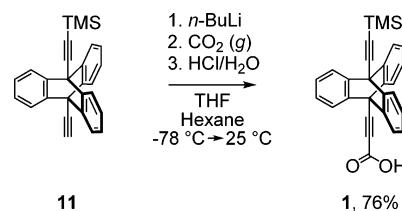
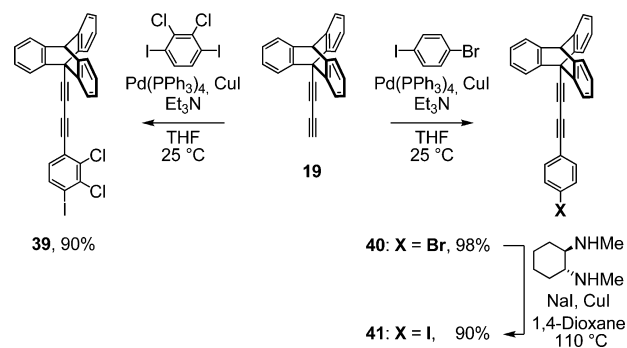
The final assembly of the molecular rotors **2** - **4** was done in three steps starting from the alkyne **7** and the rotators **23**, **24** and **28**.³⁵ Sonogashira coupling between **7** and the (hetero)aryl iodides **23**, **24**, **28** and **29** resulted in the silyl derivatives **30** - **33** in 87% to 98% yields. The terminal alkynes **34** - **37** were liberated from the silyl derivatives **30** - **33** using TBAF in THF at room temperature. Initial attempts to lithiate **34** using *n*-BuLi resulted in the dicarboxylic acid **38**, due to the acidity of the hydrogen atom located ortho to the chlorine on the dichlorophenyl rotator. The use of the weaker and sterically more demanding LiHMDS as a base in combination with substrates **35**–**37** containing CH_3 or CD_3 group in ortho position next to the chlorine or nitrogen atoms allowed their clean conversion to the desired carboxylic acids **2**–**4** (Scheme 4).

The carboxylic acid **1** containing a TMS group instead of a rotator was made by deprotonation of the alkyne **11** and trapping of the lithium acetylide with gaseous CO_2 (Scheme 5). Sonogashira coupling of **19** with an excess of 1,4-diiodo-2,3-dichlorobenzene³⁶ or 1-bromo-4-iodobenzene resulted in the halo derivatives **39** and **40** in 90% and 98% isolated yield, respectively. The less reactive **40** was converted to a more reactive iodo derivative **41** using the aromatic Finkelstein reaction (Scheme 6).

The alkyne **7** was connected with **39** or **41** using Sonogashira coupling, and the silyl derivatives **42** and **43** were obtained in nearly quantitative yields. The alkynes **44** and **45** were liberated from the silylated precursors **42** and **43** using TBAF in THF. Their deprotonation with LiHMDS followed by a reaction with ClCOOCH_3 afforded the esters **46** and **47**, which were easily purified using column chromatography. The hydrolysis of **46** and **47** by LiOH in aqueous THF afforded the desired

Scheme 4. Stepwise Construction of the Molecular Rotors **2**–**4**

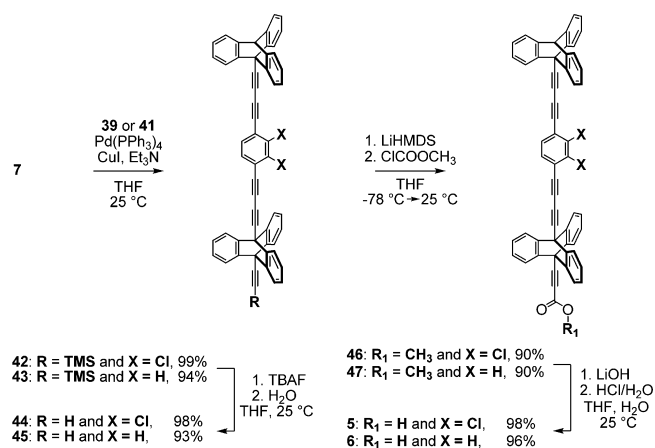
^a*n*-BuLi was used as a base. ^bLiHMDS was used as a base. ^cCompound **38** was formed exclusively.

Scheme 5. Synthesis of **1**Scheme 6. Preparation of **39** and **41**

carboxylic acids **5** and **6** in almost quantitative yield (Scheme 7).

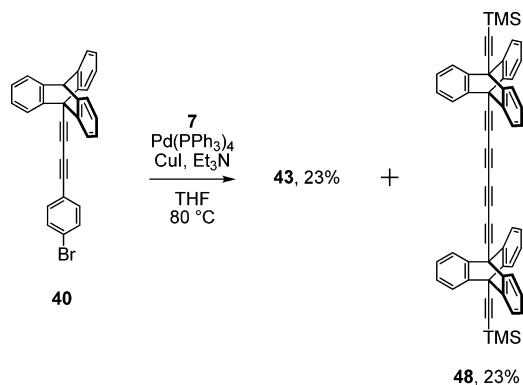
An attempted direct Sonogashira coupling of the bromo derivative **40** with the alkyne **7** required an elevated reaction temperature ($80\text{ }^{\circ}\text{C}$) and a longer reaction time, but the expected product **43** was still only formed in a synthetically

Scheme 7. Assembly of 5 and 6



useless yield (23%). A part of the starting alkyne **7** was oxidatively homocoupled to the hexayne **48** (Scheme 8).

Scheme 8. Attempted Sonogashira Coupling between 7 and 40



X-ray Crystallography. For nine of the compounds, **4**, **6**, **18**, **19**, **20**, **22**, **39**, **40**, and **48**, we were able to obtain single crystal X-ray diffraction structures. The basic crystallographic parameters are summarized in Table 1.

The ability of **19**, **20** and **22** to form a single crystal suitable for X-ray diffraction was significantly higher than that of the structurally similar compounds **7**, **16**, and **18**. We were unable to obtain useful crystals of **7** and **16**, and even after multiple attempts, compound **18** produced only low-quality crystals with disordered TMS termination. This structure is shown in Supporting Information (S155–S156) primarily to illustrate the crystal packing. Compound **20** (Supporting Information, S159–S160) suffered from similar problems due to highly disordered hydroxy groups. All attempts to grow a large single crystal of the polar double-decker structure **5** failed, but slow diffusion of pentane into a THF solution of the nonpolar analog **6** produced tiny crystals whose structure we were able to determine using synchrotron radiation.

Selected interatomic distances of these triptycene derivatives are presented in Table 2 (Figure 2). The length of the single C–C bond *a* depends on the substituent R₁ and varies from 1.338 to 1.469 Å. As expected, when located between two triple bonds, it is shorter (1.338–1.381 Å), and when connecting the triple bond *b* with a CHCBr₂ or CH₂OH group, it is longer (1.416–1.469 Å). Interatomic distances *b*, *c*, *d*, *e*, and *f* are

Table 1. Parameters of Single Crystals of 4, 6, 18, 19, 20, 22, 39, 40, and 48

cmpd	crystal system	space group	cell lengths (Å)	cell angles (°)
4	monoclinic	<i>P</i> ₂ / <i>c</i>	<i>a</i> 13.3977(8)	<i>α</i> 90
			<i>b</i> 25.4142(17)	<i>β</i> 96.447(3)
			<i>c</i> 8.1013(6)	<i>γ</i> 90
6	triclinic	<i>P</i> -1	<i>a</i> 8.1007(7)	<i>α</i> 97.056(7)
			<i>b</i> 15.4383(14)	<i>β</i> 92.982(6)
			<i>c</i> 22.617(2)	<i>γ</i> 100.618(7)
18	monoclinic	<i>P</i> ₂ / <i>c</i>	<i>a</i> 15.7725(10)	<i>α</i> 90
			<i>b</i> 20.2392(13)	<i>β</i> 93.758(3)
			<i>c</i> 8.0195(5)	<i>γ</i> 90
19	triclinic	<i>P</i> -1	<i>a</i> 11.6133(3)	<i>α</i> 85.5690(10)
			<i>b</i> 12.2509(3)	<i>β</i> 76.7590(10)
			<i>c</i> 12.4055(3)	<i>γ</i> 71.6240(10)
20	triclinic	<i>P</i> -1	<i>a</i> 8.9567(3)	<i>α</i> 98.4355(15)
			<i>b</i> 11.8107(4)	<i>β</i> 90.6462(15)
			<i>c</i> 22.4244(8)	<i>γ</i> 90.2978(15)
22	monoclinic	<i>P</i> ₂ / <i>c</i>	<i>a</i> 15.8116(7)	<i>α</i> 90
			<i>b</i> 19.4172(10)	<i>β</i> 112.850(2)
			<i>c</i> 13.1694(6)	<i>γ</i> 90
39	monoclinic	<i>P</i> ₂ / <i>n</i>	<i>a</i> 15.5042(2)	<i>α</i> 90
			<i>b</i> 13.5571(2)	<i>β</i> 109.2550(10)
			<i>c</i> 23.4410(4)	<i>γ</i> 90
40	monoclinic	<i>P</i> ₂ / <i>c</i>	<i>a</i> 9.9671(8)	<i>α</i> 90
			<i>b</i> 13.0196(13)	<i>β</i> 104.557(4)
			<i>c</i> 17.0747(14)	<i>γ</i> 90
48	triclinic	<i>P</i> -1	<i>a</i> 9.0476(4)	<i>α</i> 94.119(2)
			<i>b</i> 11.7771(6)	<i>β</i> 102.2186(19)
			<i>c</i> 13.5039(7)	<i>γ</i> 111.0808(18)

almost constant and do not change much as a function of the substituents R₁ and R₂. The length of the exocyclic bridgehead C–C bonds *c* and *e* lies between 1.447 and 1.486 Å and the interbridgehead distance *d* ranges from 2.590 to 2.639 Å. The length of the triple bonds *b* and *f* varies between 1.191 and 1.227 Å.

The crystallographic analysis also confirmed the expected flexibility of the diyne axes (Table 2). In some cases packing forces caused an arching of ordinarily straight structures (Figure 3).

In addition to providing hints concerning the possible bending of the diyne axes, the crystal structures suggest favorable modes of molecular packing, especially of the triptycene units (Supporting Information, pp S151–S168). This is of great interest for identifying the likely structures of LB monolayers.

An interesting similarity exists between the crystal packing of the rotor **6** and the hexayne **48** (Figure 4). Analogous packing was also observed in crystals of similar triptycene-based molecular rotors.^{37,38}

Langmuir–Blodgett Films. Formation of monolayers of **1** in an LB trough was facile and was examined on a variety of aqueous subphases. Solutions of MgSO₄, CaSO₄, CaCl₂, Zn(NO₃)₂, SrCl₂, and CdCl₂ yielded isotherms with molecular surface areas of 56 ± 3 Å²/molecule (type A), while pure water yielded an area of 30 ± 3 Å²/molecule (type B). Both types of isotherms are shown in Figure 5. The film of type B exhibits much less resistance to further compression.

The molecular areas can be compared with the values of 53 and 120 Å²/molecule expected from molecular modeling for the trigonal and hexagonal arrangements shown in Figure 1A,B,

Table 2. Selected Interatomic Distances and Angles in Substituted Triptycene

cmpd	R ₁ ^a	R ₂ ^a	selected interatomic distances (Å)							angles (°)	
			<i>a</i>	<i>b</i>	<i>c</i>	<i>d</i>	<i>e</i>	<i>f</i>	<i>g</i>	R ₁ - <i>x</i> - <i>y</i>	<i>x</i> - <i>y</i> - R ₂
4	CC-pyridazine-CH ₃	COOH	1.380	1.192	1.460	2.621	1.465	1.187	1.444	174.38	172.73
6	CC-Ph-CC-CC-TC ^b	COOH	1.392	1.191	1.461	2.592	1.473	1.193	1.449	175.72	179.56
	CC-Ph-CC-CC-TC-CC-COOH	–	1.338	1.227	1.486	2.590	–	–	–	176.49	–
18	CHCBr ₂	Si(CH ₃) ₃	1.441	1.191	1.455	2.639	1.454	1.216	1.814	177.78	176.63
19	CCH	–	1.378	1.200	1.460	2.608	–	–	–	172.75	–
20	CH ₂ OH	–	1.469	1.193	1.463	2.600	–	–	–	178.39	–
22	CHCBr ₂	–	1.416	1.201	1.453	2.602	–	–	–	176.76	–
39	CCPhCl ₂ I	–	1.384	1.215	1.447	2.615	–	–	–	174.36	–
40	CCPhBr	–	1.381	1.195	1.464	2.612	–	–	–	161.52	–
48	CC-CC-CC-TC-CC-Si(CH ₃) ₃	Si(CH ₃) ₃	1.368	1.201	1.462	2.629	1.461	1.202	1.842	176.65	174.76

^aItalic marked atoms were used as a reference points for evaluation of angles that describe molecular bending. ^bThe triptycene CH bridgehead was used as a reference point.

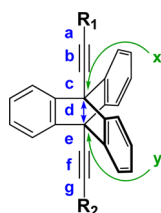


Figure 2. Labels of interatomic distances used in Table 2.

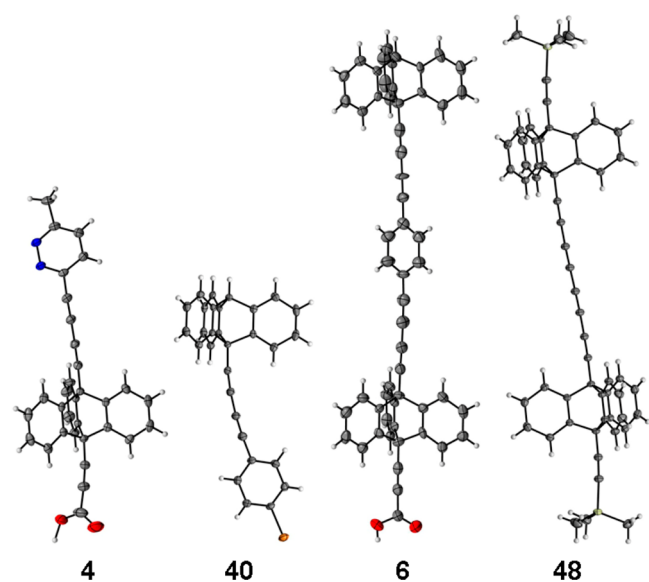


Figure 3. Single crystal X-ray structures of 4, 6, 40, and 48. ORTEPs drawn at 30% level. For additional structures, see Supporting Information, pp S151–S168.

respectively. Films of type A thus fit expectations for the trigonal arrangement, and the side view of this structure is shown in Figure 6A. We find no evidence for the hexagonal arrangement shown in Figure 1B. Molecules in films of type B must be either tilted (Figure 6B1) or packed in a double-layer arrangement (Figure 6B2) to account for the approximately halved molecular area. Proposed structures of both films are inspired by the crystal packing observed for 6 and 48 (Figure 4).

The double-layer structure presented in Figure 6 (B2) requires ca. 35 Å²/molecule, and its calculated ellipsometric thickness is ca. 15.9 Å. The monolayer thickness and the area

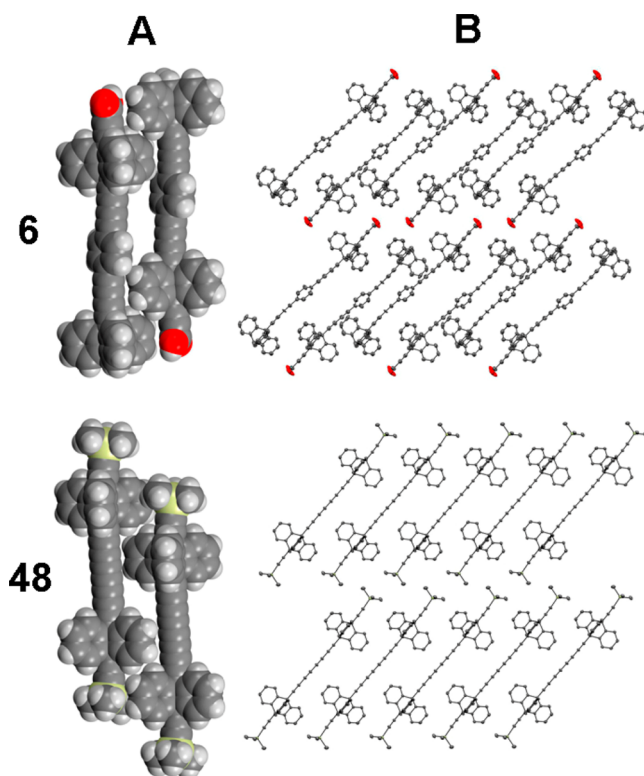


Figure 4. Single crystal X-ray structure of 6 and 48. Space-filling model of two neighboring molecules (A) and molecular packing in crystals (B). Hydrogen atoms and solvent molecules are omitted for clarity.

per molecule for film shown on Figure 6 (B1) depend on the tilt angle (Table 3).

The tilt angle of 50° represents a limiting value. It corresponds to molecules two of whose benzene rings in the triptycene unit as well as the carboxylate group touch the water surface. This structure yields a surface area of ~29 Å²/molecule and a monolayer thickness of ~8.5 Å. A reduction of the tilt angle increases the thickness of the monolayer and diminishes the area per molecule, until a second limiting value is reached at a tilt angle of ~30°. Now, the monolayer structure is forced to change dramatically, as all three benzene rings of the triptycene unit start to interact with neighboring triptycenes. Upon further reduction of the tilt angle, the area per molecule increases, as voids between molecules are generated. The monolayer thickness continues to grow. Maximum values of the area per

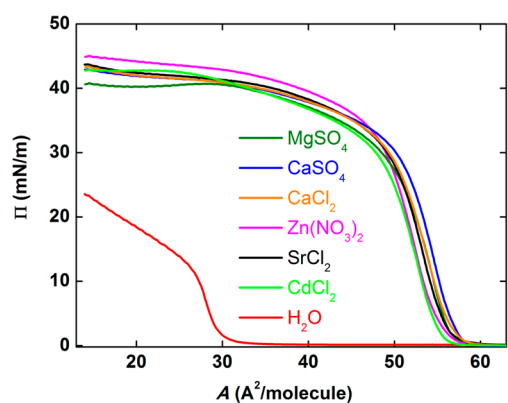


Figure 5. LB isotherms of **1** on pure water (red) and on 10 mM aqueous solutions of MgSO_4 (olive), CaSO_4 (blue), CaCl_2 (orange), $\text{Zn}(\text{NO}_3)_2$ (purple), SrCl_2 (black), and CdCl_2 (green).

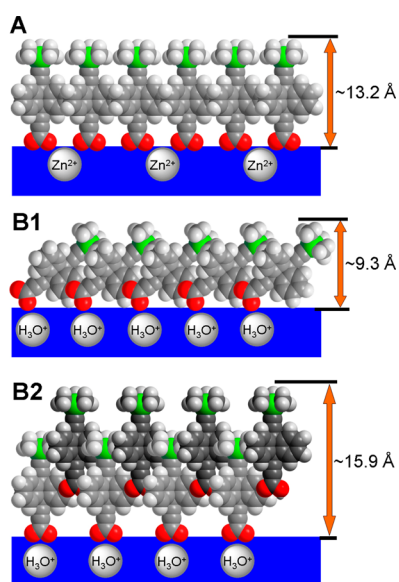


Figure 6. Proposed structures of LB films of types A and B.

molecule ($\sim 52 \text{ \AA}^2/\text{molecule}$) and of monolayer thickness (13.2 \AA) result when the tilt angle reaches zero and the molecular axes are normal to the surface.

The ellipsometric thickness measured after transfer to a gold substrate is $13.7 \pm 1.0 \text{ \AA}$ for films of type A and $9.1 \pm 1.0 \text{ \AA}$ for those of type B. The value expected from molecular modeling for a film of type A (Figure 6A) under the assumption of a straight rod oriented normal to the surface is 13.2 \AA . The value expected for the structure proposed for films of type B1 in Figure 6 is 9.3 \AA for a tilt angle 45° (Table 3) and is in good agreement with experimental observation and with crystallographic data for similarly packed **6** and **48**, whose molecules are tilted by $\sim 44^\circ$ and 39° , respectively (Figure 4B). The 15.9 \AA thickness expected for the double-layer structure shown in Figure 6B2 does not correspond to the observed value.

Water contact angle for films of type A transferred to freshly H_2 -flame cleaned Au(111) is $79 \pm 4^\circ$ and for type B is $86 \pm 4^\circ$. Both values are significantly different from the value $15\text{--}20^\circ$ observed on the bare cleaned surface, confirming the presence of a hydrophobic film.

PM-IRRAS³⁹ results measured on monolayers of type A or B transferred to an Au(111) surface were the same whether the plane of incidence of the IR light was parallel or perpendicular to the transfer direction (uniaxial sample). They compare well with the IR spectra of the lithium salt of **1** in KBr pellet (Figure 7). All peaks are at the same frequencies in both types of film,

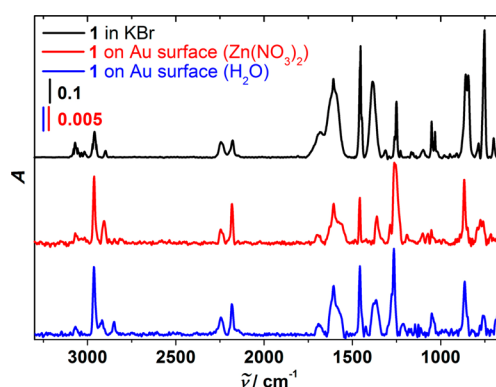


Figure 7. IR spectra of the anion of **1**: lithium salt in KBr (black) and PM-IRRAS of monolayers of type A (red) and B (blue) transferred to an Au(111) surface.

but some differ strongly in intensity. Their assignments were performed by comparison with B3LYP/6-31G(d,p) calculations for the lithium salt of **1** and with spectra of related triptycenes in which one or another functional group was absent. The solvent-free optimized geometries of the lithium salt and of the free acid **1** were unexceptional and contained straight triple bonds, but that of the free anion of **1** had a propiolate part bent $\sim 20^\circ$ away from the bridgehead-bridgehead axis. The frequency of the stretching vibration of the conjugated triple bond (2247 cm^{-1}) is higher than that of the stretching vibration of the trimethylsilylated one (2179 cm^{-1}), in agreement with previous observations on various phenylethynyl or 1,3-diethynylbicyclo[1.1.1]pentane derivatives.^{14,40,41}

Only the normal component of a transition moment of a vibration of a molecule located on a conductor surface is active, and the relative intensities of IR peaks of the anion of **1** in the monolayer transferred to the gold surface and in an isotropic sample provide information about the orientation of the IR transition moments on the surface.⁴⁴ If the IR peaks of the anion **1** can be assigned and if their polarization in the molecular framework is known, the orientation of the anion on the surface can be determined.

The analysis is particularly straightforward since the sample is uniaxial (all directions parallel to the surface are equivalent).⁴⁵ We label the normal to the surface Z and two arbitrarily chosen orthogonal directions in the plane of the surface X and Y, and introduce a molecular frame in which the three-fold symmetry

Table 3. Calculated Area per Molecule and Monolayer Thickness for a Monolayer of **1** as a Function of Tilt Angle

tilt angle ($^\circ$)	50	45	40	35	30	20	10	0
area per molecule (\AA^2)	29.0	26.8	24.4	21.7	18.9	26.3	39.0	52.2
monolayer thickness (\AA)	8.5	9.3	10.1	10.8	11.4	12.4	13.0	13.2

axis of the triptycene unit is labeled z , the line connecting the two carboxylate oxygen atoms is x , and the line perpendicular to the carboxylate plane is y . Then, using the abbreviation K_u for $\langle \cos^2 u \rangle$, where u is the angle between Z and the molecular axis u and the pointed brackets stand for averaging over all observed molecules, the absorbance E_Z for light polarized along Z is given by

$$E_Z = K_x A_x + K_y A_y + K_z A_z \quad (1)$$

where A_u is the u -polarized absorbance of the anion of **1**. The absorbance E^{iso} of the same set of molecules measured under isotropic orientation would be

$$E^{\text{iso}} = (1/3)A_x + (1/3)A_y + (1/3)A_z \quad (2)$$

The ratios $R = E_Z/E^{\text{iso}}$ are given by different expressions for longitudinal transitions polarized along z ($R_z, A_z \neq 0, A_x = A_y = 0$) and transverse transitions polarized along xy ($R_x, A_x = 0, A_y = A_z \neq 0$) or along x ($R_x, A_x = A_y = 0, A_z \neq 0$). For the moment, we assume that the plane of the carboxylate group is oriented randomly with respect to the molecular z axis, such that $K_x = K_y$ and the molecular orientation distribution is rod-like. From eqs 1 and 2, we obtain expressions 3 and 4

$$R_l = 3K_z \quad (3)$$

$$R_t = 3K_x \quad (4)$$

The absorbance measured on the LB monolayer, $I(\text{LB})$, provides a measure of E_Z . The exact isotropic absorbance E^{iso} of the same number of molecules that are observed in the monolayer is not readily available, but it is approximately proportional to the absorbance $I(\text{iso})$ of a KBr pellet containing a salt of **1**, $E^{\text{iso}} = cI(\text{iso})$, where the constant c reflects the ratio of the number of molecules observed in the LB monolayer and in the pellet. We adopt this approximation, which is likely to be good for all vibrations that do not involve the carboxylate group, and possibly reasonable even for those, if the effects of the counterion are similar in the two environments.

For purely polarized transitions, the measured ratios $R(\text{LB}/\text{iso}) = I(\text{LB})/I(\text{iso}) = cE_Z/E^{\text{iso}}$ should be equal to one of only two possible values. For longitudinal transitions:

$$R_l(\text{LB}/\text{iso}) = 3cK_z \quad (5)$$

and for transverse transitions,

$$R_t(\text{LB}/\text{iso}) = 3cK_x = (3/2)c(1 - K_z) \quad (6)$$

where we used the properties of direction cosines ($K_x + K_y + K_z = 1$). From eqs 5 and 6, we obtain an expression (7) for K_z in terms of the observed intensity ratios $R_l(\text{LB}/\text{iso})$ and $R_t(\text{LB}/\text{iso})$:

$$K_z = 1/\{1 + 2[R_t(\text{LB}/\text{iso})/R_l(\text{LB}/\text{iso})]\} \quad (7)$$

If all molecular axes z were tilted from the surface normal Z equally, their tilt angle (α) would be given by eq 8:

$$\langle \alpha \rangle = \cos^{-1} K_z^{1/2} \quad (8)$$

and $\langle \alpha \rangle$ can be viewed as the "average" tilt angle.

Performing this evaluation in practice is difficult. A potential problem that has already been mentioned is the approximation of the isotropic spectrum with a spectrum measured in a KBr pellet, where unexpected complications have been noted in the past, such as a dependence of the pellet spectrum on the grinding time.⁴⁶ We have verified that in our case the results

were unaffected by a 5-fold change in the grinding time. In addition, several problems are encountered with the measurements on the monolayer. First, intensity measurements become increasingly unreliable as peak positions drop below $\sim 1400 \text{ cm}^{-1}$, and many of the IR peaks are too weak for a reliable measurement. Second, in the laboratory atmosphere gold surface rapidly gathers aliphatic impurities whose peaks will overlap the peaks associated with the methyl groups of the anion of **1**. Third, vibrations of the carboxylate group may be affected by the presence of counterions in ways that could be different in the monolayer and in a KBr pellet. Fourth, differently polarized vibrations of the anion of **1** tend to overlap to produce peaks of mixed polarization.

This leaves a limited set of peaks that can be used for the evaluation. Fortunately, the symmetry of the anion of **1** permits only longitudinal (z) and transverse (xy or x) polarization for all vibrations (transverse vibrations that do not involve the carboxylate group are doubly degenerate and have equal transition moments in x and y directions, whereas in the absence of symmetry-lowering perturbation by the counterion the asymmetric CO stretch of the carboxylate group is polarized along x). For most of the eligible peaks the direction of polarization is obvious by inspection and agrees with the results of DFT calculations (Table 4). Starting at the highest

Table 4. IR Spectra of the Anion of **1** in KBr and in Monolayers

wavenumber (cm ⁻¹)	assignment ^{a,b}	polarization	R(LB/iso) ^{c,d}	
			type A	type B
3070	20a; CH	mixed	0.043	0.029
2960	$\nu_{\text{as}}(\text{CH}_3)$; Si-CH ₃	mixed ^e	0.086	0.108
2899	$\nu_{\text{sym}}(\text{CH}_3)$; Si-CH ₃	mixed ^e	0.110	0.100
2247	$\nu(\text{C}\equiv\text{C})$; CC-COO ⁻	longitudinal	0.057	0.087
2179	$\nu(\text{C}\equiv\text{C})$; CC-TMS	longitudinal	0.105	0.115
1610	$\nu_{\text{as}}(\text{C}=\text{O})$; COO ⁻	transverse ^f	0.011	0.027
1608	8b; Ph ring	longitudinal ^f	0.089	0.101
1454	19b; Ph ring	transverse	0.019	0.040
1383	$\nu_{\text{sym}}(\text{C}=\text{O})$; COO ⁻	longitudinal	0.016	0.017
1251	$\delta_{\text{sym}}(\text{CH}_3)$; Si-CH ₃	transverse ^e	0.148	0.137
858	$\rho(\text{CH}_3)$; Si-CH ₃	transverse ^e	0.013	0.024

^aStandard labels for aromatic vibrations (ref 42). ^bThe peak at 1655 cm⁻¹ is attributed to water (ref 43). ^cRatio $R(\text{LB}/\text{iso})$ of integrated intensities of peaks of the anion of **1** in LB film, $I(\text{LB})$, and in KBr pellet, $I(\text{iso})$: $R(\text{LB}/\text{iso}) = I(\text{LB})/I(\text{iso})$. The results are averages of four independent measurements. ^dStandard error is ± 0.006 for monolayer of Type A and ± 0.009 for monolayer of Type B. ^eThese peaks are overlapped by contributions from random impurities on the Au surface, and their intensities are unreliable. ^fA sharp peak at 1608 cm⁻¹ is overlapped with a broad peak at 1610 cm⁻¹, but they can be separated by Gaussian fitting.

frequencies, the only useful choices for longitudinally polarized transitions are the two triple bond stretches at 2247 and 2179 cm⁻¹, the aromatic ring vibration at 1608 cm⁻¹, and possibly the symmetric carboxylate vibration at 1383 cm⁻¹, if it is not too strongly perturbed by the counterion. Among the transversely polarized transitions, the asymmetric carboxylate vibration at 1610 cm⁻¹, unless perturbed by the counterion, and the aromatic ring vibration at 1454 cm⁻¹ are the only viable candidates.

In transferred monolayers of type A, the intensity of the first three longitudinally polarized vibrations is enhanced relative to their intensity in the isotropic KBr pellet and the observed $R(\text{LB}/\text{iso})$ ratios are 0.057, 0.105, and 0.089 (Table 4). Some of the differences of their $I(\text{LB})/I(\text{iso})$ ratios are undoubtedly due to measurement error, which is on the order of 0.01, but the significantly lower value of 0.057 observed for the 2247 cm^{-1} stretch of the triple bond that is closer to the surface suggests that this part of the molecule is bent and not quite perpendicular to the surface. The $I(\text{LB})/I(\text{iso})$ ratios for the two transversely polarized vibrations are similar and much smaller. The somewhat larger value for the asymmetric carboxylate stretch suggests that the line connecting the two oxygens is not exactly parallel to the surface, and this would again be compatible with the presence of a bend in the part of the molecular axis that is adjacent to the surface. The overall picture that emerges for the surface alignment of **1** in transferred monolayers of type A is that shown in Figure 6, but significantly less well ordered, probably with the anchoring group tilted away from the normal.

However, the result for the fourth vibration expected to be longitudinally polarized, the carboxylate asymmetric stretch at 1383 cm^{-1} , is in disagreement. Its $I(\text{LB})/I(\text{iso})$ ratio is much smaller than for the other three longitudinal vibrations and similar to those of transversely polarized vibrations. This result is difficult to account for, unless the counterion perturbs this carboxylate vibration differently in the Zn^{2+} salt and in the Li^+ salt. This appears likely, since we have observed a difference between the ratio of IR intensities of the carboxylate bands in the spectra of AcOLi and $(\text{AcO})_2\text{Zn}\cdot 2\text{H}_2\text{O}$ in a KBr pellet. We conclude that the 1383 cm^{-1} vibration cannot be used in the determination of molecular orientation.

If we use the average values of the $I(\text{LB})/I(\text{iso})$ ratio for the apparently most reliably determined longitudinal vibrations at 2179 and 1608 cm^{-1} and transverse vibrations at 1610 and 1454 cm^{-1} along with their statistical uncertainties, we obtain an average tilt angle of $29 \pm 4^\circ$ for molecular axes in the film transferred from a subphase containing Zn^{2+} cations. In monolayers of type B, transferred from pure water, a similar procedure yields an average tilt angle of $38 \pm 4^\circ$.

DISCUSSION

Synthesis. The synthesis of the triptycene derivatives **1–6** proceeded as expected, and only a few observations require comments. The generality of the synthetic approach is apparent, because the singly protected alkyne **7** could in principle be coupled with almost any (hetero)aryl bromide, iodide, or triflate, providing access to a variety of molecular rotors with different dipolar rotators.

The commonly isolated yield of the triptycene **10** from the Diels–Alder addition of benzyne to the disubstituted anthracene **9** was $\sim 23\%$. In contrast, the yield was usually 35% when the monosubstituted anthracene **13** was used as a starting material. The presence of two ethynyl groups in **9** probably makes this structure more vulnerable to side reactions, either polymerization or 2 + 2 benzyne cycloaddition. The products of TMS cleavage were not isolated from the complex reaction mixtures.

The TMS-substituted derivatives **30–33** were in general significantly more soluble than the corresponding free alkynes **34–37**, presumably due to the more effective crystal packing of the latter.

X-ray Crystallography. The single-crystal X-ray diffraction results serve two purposes. First, the intramolecular structural data (Table 2, Figure 3) help us to estimate the likely degree of deviation from planarity that the diyne axes tolerate. Second, the intermolecular interactions revealed by crystal packing (Figure 4) provide hints for the likely structures of the LB films generated now from **1** and later, from its congeners **2–6**.

The observed significant bending of the diyne rotor axle represents a clear warning that its flexibility may be excessive for the intended use in molecular rotors and that a single triple bond or another type of connector may be preferable for the purpose. The most extreme case was observed in **40** where the position of the benzene ring deviates by almost 20° from the axis defined by the two triptycene bridgehead carbons x and y (Figures 2 and 3). The long tetrayne **48** and the rotor **6** are S-shaped, as is fairly common in conjugated polyynes.⁴⁷

The crystal packing observed for several of the triptycenes studied presently, and for others reported in the literature,^{14,34,35} is suggestive. In a crystal, the triptycene subunits do not spontaneously pack in the manner shown in Figure 1, with the triptycene cores in a common plane, but prefer to be displaced, as shown in Figure 4. In the crystals of both **6** and **48**, the molecular axes are parallel, but the triptycenes are not interlocked. Instead, the triple bonds are nestled between two paddles of a triptycene carried by a neighboring molecule. The interlocked structure of Figure 1 could perhaps be found in crystals in which it is enforced by some additional factors that discourage the arrangement shown in Figure 4 and favor the placement of all the triptycenes in a single plane.

The easy bending of the rotor axle and the reluctance of the triptycene units to locate in a single plane suggest that transfer of the LB film from the aqueous subphase to a solid substrate could easily be associated with considerable changes in film structure and that the ellipsometric thickness observed after transfer may not be fully representative of the thickness on the water surface.

Langmuir–Blodgett Monolayers. The sensitivity of the LB behavior of **1** to the nature of the subphase is striking. We propose that it reflects a competition between two factors: (i) The natural tendency of the alkynyltriptycene structures to nestle their triple bonds or whole trimethylsilylethynyl groups between two of the corner-forming aromatic rings of a neighboring triptycene as illustrated in Figure 4; and (ii) the tendency of divalent cations present in the aqueous subphase to hold two neighboring ionized carboxylate groups in perpendicular position to water surface, thus forcing all the molecules to adopt the orientation shown in Figure 6A. Based on the observed values of 53 and 30 \AA^2 for area per molecule and the expectations shown in Table 3, we propose that (i) on subphases containing divalent cations, the latter tendency prevails, and in monolayers of type A the axes are roughly normal to the surface; and (ii) on pure water, the former tendency does, and the axes are tilted at approximately 50° . The resulting tentatively proposed structure of a film of type A is shown in Figure 6A, while that of a film of type B is shown in Figure 6B1. The low resistance of the films of type B1 to further compression is most likely a reflection of the ease with which some molecules can slide under already existing film, forming triple and higher multiple layers. The accuracy of the estimated tilt angles is undoubtedly poor, since they are based merely on molecular modeling. Some comfort can be derived from the observation that the tilt angle deduced for films of

type B is very close to angles observed in single crystals of the related triptycenes **6** and **48**.

Additional support for the tilted structure of monolayers of type B can be derived from observations of thickness and IR intensities after transfer to a gold surface. It seems that the transfer has little if any effect on the structure, in that the ellipsometric thickness is best accommodated by a tilt angle of 45° (Table 3) and the IR data produce a value of 38°. The interpretation of the data obtained for transferred monolayers of type A is more difficult. The ellipsometric thickness of 13.7 Å is within the anticipated error of the value 13.2 Å expected from modeling for molecules that are not tilted at all, whereas the IR data suggest a tilt angle of 29°. The ellipsometric thickness may be exaggerated since it does not only include the length of the molecule of **1** but also the Zn²⁺ cations and water, and we tend to place more faith in the IR result and suspect that the transfer to a solid substrate causes some tilt of the molecular axes.

For the purposes of the planned new approach to triangular arrays of dipolar molecular rotors, we conclude that the LB study of the model compound **1** proved that conditions conducive to the formation of stable monolayers with interlocked triptycenes can be found but that there is significant danger that after transfer to a solid substrate the rotor axes will not be normal to the surface as desired. It appears worthwhile to subject monolayers formed from compounds **2–6** to a thorough examination, both before and after transfer to a solid substrate.

CONCLUSION

We designed, synthesized, and characterized several triptycene-based molecular rotors for the preparation of trigonally organized LB films. These molecules differ in length, dipolar rotators (2,3-dichlorophenyl and 3-pyridazinyl), and numbers of triptycene units. For the simplest of these molecular rotors (**1**), we demonstrated monolayer formation and transferability and obtained evidence compatible with the expected trigonal structure. It remains to be seen whether in monolayers transferred to a solid substrate if the rotor axes will be perpendicular to the surface as desired.

EXPERIMENTAL SECTION

Materials. All reactions were carried out under argon atmosphere with dry solvents freshly distilled under anhydrous conditions, unless otherwise noted. Standard Schlenk and vacuum line techniques were employed for all manipulations of air- or moisture-sensitive compounds. Yields refer to isolated, chromatographically and spectroscopically homogeneous materials, unless otherwise stated.

9-Trimethylsilylethynyl-10-ethynyltriptycene (**11**) was synthesized according to a previously published procedure.¹⁴ THF and ether were dried over sodium with benzophenone and distilled under argon prior to use. Triethylamine and CH₂Cl₂ were dried over CaH₂ and distilled under argon prior to use. All other reagents were used as supplied unless otherwise stated. Chloroform was dried over P₄O₁₀ and distilled under argon prior to use.

Procedures. Analytical thin-layer chromatography (TLC) was performed using precoated TLC aluminum sheets (Silica gel 60 F₂₅₄). TLC spots were visualized using either UV light (254 nm) or a 5% solution of phosphomolybdic acid in ethanol and heat (200 °C) as a developing agent. Flash chromatography was performed using silica gel (high purity grade, pore size 60 Å, 70–230 mesh). Melting points are reported uncorrected. Infrared spectra (IR) were recorded in KBr pellets. Chemical shifts in ¹H, ²H, and ¹³C NMR spectra are reported in ppm on the δ scale relative to CHCl₃ (δ = 7.26 ppm for ¹H NMR), CHCl₃ (δ = 77.0 ppm for ¹³C NMR), THF-*d*₆ (δ = 1.72 and 3.58 ppm for ¹H NMR), THF-*d*₆ (δ = 25.40 and 67.50 ppm for ¹³C NMR),

acetone-*d*₆ (δ = 2.05 ppm for ¹H NMR), and acetone-*d*₆ (δ = 29.8 and 206.3 ppm for ¹³C NMR) as internal references. Splitting patterns are assigned s = singlet, d = doublet, t = triplet, m = multiplet, br = broad signal. Some carbon signals of CD₃ groups were not detected due to strong ¹³C–²H coupling. The content of ²H was determined by elemental analysis as ¹H since this method is not able to recognize the difference between ²H and ¹H.

High-resolution mass spectra (HRMS) using atmospheric-pressure chemical ionization (APCI) and electrospray ionization (ESI) were obtained on a mass analyzer combining linear ion trap and the Orbitrap, and those using electron ionization (EI) and chemical ionization (CI) mode were taken on a time-of-flight mass spectrometer.

Molecular Modeling and Calculations. Molecular models were generated using ChemBio3D Ultra 11.0 software.⁴⁸ Starting structure for **1** was drawn in ChemDraw and Cartesian coordinates were obtained from ChemBio3D Ultra 11.0 software. Geometry was optimized, and IR frequencies and transition moments were calculated using density functional theory (DFT) at the B3LYP/6-31G(d,p) level using Gaussian 09.⁴⁹

X-ray Diffraction. Crystallographic data for **4**, **18**, **19**, **20**, **22**, **39**, **40**, and **48** were collected on a Kappa geometry diffractometer equipped with CCD detector by monochromatized MoK_α radiation (λ = 0.71073 Å) at a temperature of 150(2) K. The structures were solved by direct methods (SHELXS)⁵⁰ and refined by full matrix least-squares based on F² (SHELXL97).⁴⁷

Crystallographic data for **6** were acquired on diffractometer with a PHOTON100 CMOS detector running shutterless at the Advance Light Source beamline 11.3.1 using a Silicon(111) monochromatized synchrotron radiation (λ = 0.7749 Å) at a temperature of 100(2) K.

Langmuir–Blodgett Films. Langmuir film experiments were performed with a LB trough system using either pure water or 10 mM aqueous solution of MgSO₄, CaSO₄, CaCl₂, Zn(NO₃)₂, SrCl₂, and CdCl₂ as a subphase at room temperature. A 0.53 mg/mL solution of **1** in chloroform (50 μL) was added dropwise from a microsyringe, and the solvent was allowed to evaporate during ~10 min. Compression isotherms were recorded at 10 mm/min barrier speed using software that was provided with the KSV instrument. Transfer to a butane-flamed Au(111) surface occurred with a transfer ratio of 1.0 ± 0.2.

Monolayer Characterization. Ellipsometric thickness was determined with Stokes ellipsometer with a 633 nm HeNe laser with the incident angle adjusted to 70°, assuming an index of refraction equal to 1.47. Contact angle was determined with a contact angle goniometer. PM-IRRAS were recorded using a FT-IR spectrometer with a PEM module including a nitrogen cooled mercury–cadmium–telluride (MCT) detector and a ZnSe photoelastic modulator. The IR beam was set at 78° incident to the Au surface, and the spectra were collected over 90 min with a resolution of 4 cm⁻¹. All measurements of ellipsometric thickness, contact angle, and IR spectra were repeated three times for each sample.

Synthesis. 3-(10-Trimethylsilylethynyl-triptycen-9-yl)propionic Acid (**1**). A solution of *n*-BuLi in hexane (2.5 M, 144 μL, 0.360 mmol) was added dropwise to a stirred solution of **11** (90 mg, 0.240 mmol) in THF (15 mL) at –78 °C. The slightly yellowish solution was stirred at –78 °C for 30 min. Gaseous CO₂ was bubbled into the solution through a PTFE cannula at –78 °C for 20 min and at room temperature for additional 10 min. A dense white solid precipitated. The white suspension was diluted with water (30 mL), acidified with concentrated HCl (pH ≈ 1), extracted with ether (4 × 30 mL), and combined colorless ethereal phases were dried over MgSO₄. Solvents were removed under reduced pressure. The slightly yellowish solid residue was triturated with an ice-cold hexane (1 × 3 mL) and dried using Kugelrohr distillation apparatus (90 °C, 500 mTorr, 60 min). Carboxylic acid **1** was obtained as a white crystalline solid (76 mg, 0.182 mmol, 76%).

Mp 219 °C (dec.). ¹H NMR (400 MHz, CDCl₃): δ 0.49 (s, 9H), 7.15–7.17 (m, 6H), 7.72–7.78 (m, 6H), 9.68 (br s, 1H). ¹³C NMR (100 MHz, CDCl₃): δ 0.3, 52.1, 53.1, 83.5, 85.1, 98.5, 99.0, 121.9, 122.6, 126.0, 126.2, 141.8, 143.0, 157.3. IR (KBr): 3427, 3070, 3034, 3017, 2960, 2899, 2247, 2179, 2146, 1730, 1692, 1608, 1486, 1455,

1446, 1411, 1309, 1281, 1261, 1250, 1219, 1168, 1156, 1140, 1096, 1051, 1033, 1005, 978, 947, 856, 844, 752, 693, 664, 652, 640, 627, 599, 553, 486 cm^{-1} . MS, m/z (%): 417.2 (9, M - H), 373.2 (100, M - COOH), 345.1 (18, M - TMS). HRMS, (ESI-) for $(\text{C}_{28}\text{H}_{21}\text{O}_2\text{Si}^-)$: calcd 417.13163, found 417.13155. Anal. calcd for $\text{C}_{28}\text{H}_{22}\text{O}_2\text{Si}$: C, 80.35; H, 5.30. Found: C, 80.02; H, 5.33.

Rotor 2. A solution of *n*-BuLi in hexane (2.5 M, 138 μL , 0.346 mmol) was added dropwise to a stirred solution of **35** (140 mg, 0.288 mmol) in THF (5 mL) at -78°C . The slightly yellowish solution was stirred at -78°C for 30 min. Gaseous CO_2 was bubbled into the solution through a PTFE cannula at -78°C for 10 min and at room temperature for additional 10 min. The reaction mixture was diluted with water (15 mL), acidified with concentrated HCl ($\text{pH} \approx 1$), and extracted with CH_2Cl_2 (3×20 mL), and combined colorless organic phases were dried over MgSO_4 . Solvents were removed under reduced pressure, and the yellowish solid residue was recrystallized from boiling ethanol. Crystals were filtered on frit, subsequently washed with ice-cold ethanol (2×4 mL), and thoroughly dried using Kugelrohr distillation apparatus (90°C , 500 mTorr, 60 min). Rotor 2 was obtained as a white crystalline solid (130 mg, 0.246 mmol, 85%). A sample for elemental analysis was crystallized from THF.

Mp $> 290^\circ\text{C}$ (dec.). ^1H NMR (400 MHz, THF- d_6): δ 2.47 (s, 3H), 7.14–7.16 (m, 6H), 7.33 (d, $J = 8.15$ Hz, 1H), 7.63 (d, $J = 7.93$ Hz, 1H), 7.71–7.75 (m, 6H), 12.36 (br s, 1H). ^{13}C NMR (100 MHz, THF- d_6): δ 21.5, 53.1, 54.2, 75.8, 77.6, 78.6, 79.8, 80.3, 86.7, 121.8, 123.0, 123.1, 127.1, 127.2, 130.1, 133.2, 134.3, 136.2, 141.6, 143.4, 143.8, 154.2. IR (KBr): 3070, 3033, 3017, 2957, 2922, 2247, 1727, 1692, 1606, 1486, 1458, 1454, 1443, 1413, 1369, 1343, 1305, 1282, 1247, 1238, 1218, 1156, 1141, 1126, 1101, 1066, 1033, 1014, 979, 952, 909, 868, 816, 782, 755, 732, 639, 624 cm^{-1} . MS, m/z (%): 527.1 (9, M - H), 483.1 (100, M - COOH). HRMS, (ESI-) for $(\text{C}_{34}\text{H}_{17}\text{Cl}_2\text{O}_2^-)$: calcd 527.06111, found 527.06104. Anal. calcd for $\text{C}_{34}\text{H}_{18}\text{Cl}_2\text{O}_2 + \text{THF}$ in 1:1 ratio: C, 75.88; H, 4.36. Found: C, 75.75; H, 4.70.

Rotor 3. A solution of **36** (125 mg, 0.256 mmol) in THF (20 mL) was slowly added to a stirred solution of LiHMDS at -78°C , freshly prepared from TMS_2NH (160 μL , 0.768 mmol) in THF (8 mL) and *n*-BuLi in hexane (2.5 M, 266 μL , 0.666 mmol). The colorless solution was stirred at -78°C for 30 min. Gaseous CO_2 was bubbled into the solution through a PTFE cannula at -78°C for 10 min and at room temperature for additional 10 min. A dense white solid precipitated. The suspension was diluted with 20% aqueous NaHCO_3 (50 mL) and washed with ether (2×30 mL). A clear aqueous phase was acidified with concentrated HCl ($\text{pH} \approx 1$) (a dense white solid precipitated) and extracted with CH_2Cl_2 (6×20 mL), and combined colorless organic phases were dried over MgSO_4 . Solvent was removed under reduced pressure, and the yellowish solid residue was recrystallized from boiling ethanol. Crystals were filtered on frit, subsequently washed with ice-cold ethanol (2×4 mL), and thoroughly dried using Kugelrohr distillation apparatus (110°C , 500 mTorr, 120 min). Rotor 3 was obtained as a white crystalline solid (98 mg, 0.184 mmol, 72%).

Mp $> 290^\circ\text{C}$ (dec.). ^1H NMR (400 MHz, THF- d_8): δ 7.14–7.16 (m, 6H), 7.32 (d, $J = 7.94$ Hz, 1H), 7.63 (d, $J = 7.94$ Hz, 1H), 7.71–7.76 (m, 6H), 12.30 (br s, 1H). ^2H NMR (76 MHz, THF- h_8): δ 2.45 (s, 3D). ^{13}C NMR (100 MHz, THF- d_8): δ 20.8 (sep, $J_{\text{C,D}} = 19.6$ Hz), 53.1, 54.2, 75.8, 77.6, 78.6, 79.8, 80.4, 86.7, 121.8, 123.0, 123.1, 127.1, 127.2, 130.1, 133.2, 134.3, 136.2, 141.5, 143.3, 143.8, 154.2. IR (KBr): 3070, 3034, 3017, 2985, 2966, 2249, 1747, 1695, 1645, 1606, 1485, 1454, 1442, 1415, 1369, 1341, 1307, 1281, 1252, 1239, 1157, 1141, 1129, 1066, 1033, 1005, 980, 878, 857, 822, 797, 751, 717, 650, 638, 623, 615, 571, 490, 477 cm^{-1} . MS, m/z (%): 530.1 (10, M - H), 486.1 (100, M - COOH). HRMS, (ESI-) for $(\text{C}_{34}\text{H}_{14}\text{H}_3\text{Cl}_2\text{O}_2^-)$: calcd 530.07994, found 530.07988. Anal. calcd for $\text{C}_{34}\text{H}_{15}\text{H}_3\text{Cl}_2\text{O}_2$: C, 76.70; H, 3.42. Found: C, 76.43; H, 3.63.

Rotor 4. A solution of **37** (150 mg, 0.358 mmol) in THF (20 mL) was slowly added to a stirred solution of LiHMDS at -78°C , freshly prepared from TMS_2NH (112 μL , 0.537 mmol) in THF (10 mL), and *n*-BuLi in hexane (2.5 M, 186 μL , 0.465 mmol). The slightly orange solution was stirred at -78°C for 30 min. Gaseous CO_2 was bubbled into the solution through a PTFE cannula at -78°C for 10 min and at

room temperature for additional 10 min. A dense white solid precipitated. Suspension was diluted with 20% aqueous NaHCO_3 (50 mL) and washed with ether (2×30 mL). A clear colorless aqueous phase was carefully acidified with concentrated HCl ($\text{pH} \approx 4-5$) (a dense white solid precipitated) and extracted with CH_2Cl_2 (3×25 mL), and combined colorless organic phases were dried over MgSO_4 . Solvent was removed under reduced pressure, and the yellowish solid residue was recrystallized from boiling ethanol. Crystals were filtered on a frit, subsequently washed with ice-cold ethanol (2×4 mL), CHCl_3 (3×3 mL), and thoroughly dried using Kugelrohr distillation apparatus (90°C , 500 mTorr, 30 min). Rotor 4 was obtained as a white crystalline solid (116 mg, 0.251 mmol, 70%).

Mp $> 200^\circ\text{C}$ (dec.). ^1H NMR (400 MHz, THF- d_8): δ 2.72 (s, 3H), 7.13–7.18 (m, 6H), 7.49 (dd, $J_1 = 0.45$ Hz, $J_2 = 8.55$ Hz, 1H), 7.71–7.74 (m, 3H), 7.75–7.77 (m, 3H), 7.78 (dd, $J_1 = 0.21$ Hz, $J_2 = 8.54$ Hz, 1H), 12.36 (br s, 1H). ^{13}C NMR (100 MHz, THF- d_8): δ 22.5, 53.1, 54.2, 76.0, 76.7, 77.4, 79.7, 80.3, 86.7, 123.0, 123.1, 126.6, 127.20, 127.21, 131.0, 143.3, 143.7, 145.6, 154.2, 160.0. IR (KBr): 3069, 3052, 3016, 2243, 2162, 1723, 1606, 1583, 1542, 1485, 1455, 1444, 1419, 1348, 1306, 1279, 1243, 1155, 1140, 1126, 1096, 1063, 1033, 954, 941, 922, 860, 837, 816, 778, 760, 721, 670, 649, 639, 614 cm^{-1} . MS, m/z (%): 485.2 (28, M + Na), 463.2 (100, M + H). HRMS, (ESI+) for $(\text{C}_{32}\text{H}_{18}\text{N}_2\text{O}_2 + \text{H}^+)$: calcd 463.14410, found 463.14405. Anal. calcd for $\text{C}_{32}\text{H}_{18}\text{N}_2\text{O}_2$: C, 83.10; H, 3.92; N, 6.06. Found: C, 83.39; H, 3.99; N, 5.67.

"Double Decker" Rotor 5. To a solution of ester **46** (200 mg, 0.241 mmol) in THF (16 mL) was added a solution of $\text{LiOH}\cdot\text{H}_2\text{O}$ (152 mg, 3.615 mmol) in water (4 mL) at room temperature. The clear yellowish mixture was stirred for 3 h at room temperature. THF was removed under reduced pressure, and the white suspension was diluted with water (5 mL). The aqueous phase was acidified with concentrated HCl ($\text{pH} \approx 1$), a dense white precipitate was filtered on a frit, subsequently washed with deionized water (3×3 mL), hexane (3×5 mL), mixture of hexane and CH_2Cl_2 in 3:1 ratio (3×5 mL), once again with hexane (3×5 mL), and finally thoroughly dried using Kugelrohr distillation apparatus (40 min, 80°C , 600 mTorr). Rotor 5 was obtained as a white crystalline solid (192 mg, 0.235 mmol, 98%).

Mp $> 300^\circ\text{C}$ (dec.). ^1H NMR (500 MHz, THF- d_8): δ 5.55 (s, 1H), 7.02–7.08 (m, 6H), 7.14–7.18 (m, 6H), 7.42–7.43 (m, 3H), 7.68–7.70 (m, 3H), 7.73–7.76 (m, 6H), 7.81 (s, 2H), 12.06 (br s, 1H). ^{13}C NMR (125 MHz, THF- d_8): δ 53.1, 54.0, 54.3, 54.9, 74.8, 75.2, 76.7, 77.3, 80.2, 81.5, 81.7, 81.9, 83.0, 86.8, 122.8, 123.06, 123.08, 124.6, 125.2, 125.5, 126.1, 126.9, 127.20, 127.22, 133.6, 136.91, 136.92, 143.3, 143.7, 144.8, 145.6, 154.3. IR (KBr): 3069, 3017, 2958, 2868, 2245, 2159, 1736, 1694, 1607, 1581, 1455, 1409, 1369, 1330, 1275, 1239, 1152, 1143, 1128, 1104, 1064, 1033, 1027, 977, 946, 859, 827, 809, 751, 639, 627, 606, 550, 524, 480 cm^{-1} . MS, m/z (%): 813.1 (32, M - H), 769.1 (100, M - COOH). HRMS, (ESI-) for $(\text{C}_{57}\text{H}_{27}\text{Cl}_2\text{O}_2^-)$: calcd 813.13936, found 813.13892. Anal. calcd for $\text{C}_{57}\text{H}_{28}\text{Cl}_2\text{O}_2$: C, 83.93; H, 3.46. Found: C, 83.88; H, 3.58.

"Double Decker" Rotor 6. To a solution of ester **47** (250 mg, 0.329 mmol) in THF (16 mL) was added a solution of $\text{LiOH}\cdot\text{H}_2\text{O}$ (140 mg, 3.337 mmol) in water (4 mL) at room temperature. The clear yellowish mixture was stirred for 3 h at room temperature. THF was removed under reduced pressure, and a white suspension was diluted with water (5 mL). The aqueous phase was acidified with concentrated HCl ($\text{pH} \approx 1$), a dense white precipitate was filtered on frit, subsequently washed with deionized water (3×3 mL), hexane (3×5 mL), mixture of hexane and CH_2Cl_2 in 3:1 ratio (3×5 mL), once again with hexane (3×5 mL), and finally thoroughly dried using Kugelrohr distillation apparatus (60 min, 80°C , 600 mTorr). The carboxylic acid **6** was obtained as a white crystalline solid (235 mg, 0.315 mmol, 98%).

Mp $> 310^\circ\text{C}$ (dec.). ^1H NMR (500 MHz, THF- d_8): δ 5.54 (s, 1H), 7.01–7.07 (m, 6H), 7.14–7.18 (m, 6H), 7.41–7.42 (m, 3H), 7.68–7.69 (m, 3H), 7.72–7.76 (m, 6H), 7.77 (s, 4H). ^{13}C NMR (100 MHz, THF- d_8): δ 53.1, 54.0, 54.2, 54.9, 76.4, 76.8, 77.2, 77.8, 78.4, 78.9, 79.3, 80.3, 80.5, 86.7, 122.8, 123.0, 123.1, 123.4, 123.8, 124.5, 126.0, 126.8, 127.2, 133.92, 133.93, 143.4, 143.9, 145.0, 145.6, 154.3. IR (KBr): 3069, 3036, 3017, 2957, 2246, 1732, 1699, 1608, 1508, 1457,

1403, 1338, 1304, 1288, 1267, 1237, 1188, 1155, 1104, 1082, 1034, 1026, 945, 860, 838, 749, 693, 676, 639, 623, 607, 545 cm⁻¹. MS, *m/z* (%): 745.2 (34, M - H), 701.2 (100, M - COOH). HRMS, (ESI-) for (C₅₇H₂₉O₂⁻): calcd 745.21730, found 745.21710. Anal. calcd for C₅₇H₃₀O₂ + H₂O in 2:1 ratio: C, 90.57; H, 4.13. Found: C, 90.41; H, 4.12.

9-Trimethylsilylethynyl-10-(buta-1,3-dienyl)triptycene (7). The solution of *n*-BuLi in hexane (2.5 M, 3.98 mL, 9.939 mmol) was added dropwise to a solution of **18** (1.850 g, 3.313 mmol) in THF (35 mL) cooled at -78 °C. A dense white precipitate formed. The suspension was stirred at -78 °C for 2.5 h. Subsequently, concentrated aqueous NH₄Cl (10 mL) was added, and cooling was discontinued. The yellow reaction mixture was diluted with ether (150 mL) and washed with saturated aqueous NH₄Cl (2 × 40 mL). Clear yellowish organic phase was dried over MgSO₄, and volatiles were removed under reduced pressure. Column chromatography on silica gel (hexane/CH₂Cl₂, 5:1) gave **7** as a white crystalline solid (1.247 g, 3.129 mmol, 94%).

Mp > 200 °C (dec.). ¹H NMR (400 MHz, CDCl₃): δ 0.50 (s, 9H), 2.43 (s, 1H), 7.13–7.15 (m, 6H), 7.73–7.77 (m, 6H). ¹³C NMR (100 MHz, CDCl₃): δ 0.3, 52.5, 52.9, 67.7, 68.5, 71.5, 76.3, 98.3, 99.2, 122.0, 122.4, 125.8, 125.9, 142.8, 143.0. IR (KBr): 3303, 3293, 3071, 3035, 3017, 2959, 2898, 2248, 2232, 2182, 2168, 1608, 1454, 1443, 1423, 1408, 1307, 1251, 1231, 1167, 1159, 1118, 1055, 1032, 976, 951, 874, 843, 751, 743, 699, 659, 640, 631, 495, 480 cm⁻¹. MS, *m/z* (%): 398.1 (100, M), 383.1 (25, M - CH₃), 367.1 (12), 348.1 (7), 339.1 (14), 324.1 (39, M - TMS), 313.1 (5), 300.1 (31), 289.1 (5), 276.1 (12), 252.1 (6), 73.0 (27, TMS). HRMS, (EI) for (C₂₉H₂₂Si⁺): calcd 398.1491, found 398.1498. Anal. calcd for C₂₉H₂₂Si: C, 87.39; H, 5.56. Found: C, 87.05; H, 5.50.

9-(Trimethylsilylethynyl)anthracene (13).²⁹ A previously published procedure²⁹ was adapted as follows: A flame-dried and argon filled apparatus consisting of 500 mL two-necked flask equipped with a gas condenser and magnetic stirrer was charged with 9-bromoanthracene (**12**) (25.000 g, 97.227 mmol), PdCl₂(PPh₃)₂ (2.730 g, 3.889 mmol, 4 mol %), and CuI (0.556 g, 2.917 mmol, 3 mol %). After five successive vacuum/argon cycles, dry and degassed Et₃NH (400 mL) was cannulated to the reaction mixture. Finally, trimethylsilylacetylene (20.6 mL, 145.841 mmol) was added from a syringe. The reaction mixture turned black immediately. The dark solution was stirred for 20 h at 100 °C. A dense dark solid precipitated. All volatiles were removed under reduced pressure, and a black oily residue was suspended in ether (1 L). The dark organic phase was extracted with water (1 × 200 mL) and saturated aqueous NH₄Cl (2 × 300 mL), and the combined aqueous phases were extracted with ether (3 × 200 mL). The combined ethereal phases were dried over MgSO₄, and volatiles were removed under reduced pressure. Column chromatography on silica gel (hexane/CH₂Cl₂, 10:1) gave **13** as a yellow crystalline solid (25.290 g, 92.155 mmol, 95%).

¹H NMR (400 MHz, CDCl₃): δ 0.43 (s, 9H), 7.50 (ddd, *J*₁ = 1.11 Hz, *J*₂ = 6.54 Hz, *J*₃ = 8.10 Hz, 2H), 7.59 (ddd, *J*₁ = 1.14 Hz, *J*₂ = 6.47 Hz, *J*₃ = 8.26 Hz, 2H), 8.00 (dd, *J*₁ = 0.55 Hz, *J*₂ = 8.44 Hz, 2H), 8.42 (s, 1H), 8.56 (ddd, *J*₁ = 0.89 Hz, *J*₂ = 1.87 Hz, *J*₃ = 8.68 Hz, 2H). ¹³C NMR (400 MHz, CDCl₃): δ 0.3, 101.5, 106.2, 117.1, 125.6, 126.7, 126.8, 127.9, 128.6, 131.0, 132.9, in agreement with literature.²⁹

9-(Trimethylsilylethynyl)triptycene (14).³⁰ A previously published procedure³⁰ was adapted as follows: A solution of **13** (23.000 g, 83.810 mmol) in anhydrous DME (400 mL) was cannulated into a flame-dried and argon-filled 1 L three-necked flask equipped with a gas condenser, stirrer, and two 250 mL dropping funnels. Isoamyl nitrite (90.0 mL, 670.0 mmol) was dissolved in DME (100 mL) and placed into the first dropping funnel. The second dropping funnel was filled with solution of anthranilic acid (68.981 g, 503.000 mmol) in DME (150 mL). The solution in the reaction flask was magnetically stirred and heated to gentle reflux (~100 °C) using heating mantle with magnetic stirrer. The two solutions in the funnels were slowly dropped into the reaction vessel at the same rate over 6 h. The addition of the solutions was accompanied by rapid evolution of gases (CO₂ and N₂). The reaction mixture turned black during that time and was refluxed for an additional 16 h. All volatiles were removed under reduced pressure,

and a dark honey-like residue was triturated with boiling hexane (8 × 250 mL). Hexane was evaporated, and remaining high boiling species were removed under reduced pressure (150 °C, 500 mTorr). (Note: It is crucial to remove all volatiles - mostly isoamyl nitrite and products of its decomposition - to get sufficient separation during subsequent column chromatography.) A black solid residue was sorbed on silica gel (20 g) and placed on a column filled with silica gel (500 g). Slow elution (hexane) provided **14** as a white or slightly yellowish solid (10.169 g, 29.010 mmol, 35%).

¹H NMR (400 MHz, CDCl₃): δ 0.49 (s, 9H), 5.43 (s, 1H), 7.03–7.11 (m, 6H), 7.39–7.41 (m, 3H), 7.73–7.75 (m, 3H). ¹³C NMR (400 MHz, CDCl₃): δ 0.4, 53.2, 53.7, 97.6, 100.0, 122.4, 123.3, 125.1, 125.6, 144.1, 144.4, in agreement with literature.³⁰

9-Ethynyltriptycene (15).³⁰ To an ice-cold and well stirred solution of **14** (10.169 g, 29.010 mmol) in wet THF (60 mL) was slowly dropwise added a solution of TBAF in THF (1.0 M, 30.0 mL, 30.000 mmol). The brownish-red reaction mixture was stirred at room temperature for 30 min. It was then diluted with ether (200 mL) and washed with water (3 × 40 mL), and the organic phase was dried over MgSO₄. Solvents were removed under reduced pressure and column chromatography on a silica gel (hexane/CH₂Cl₂, 3:1) afforded **15** as a white crystalline solid (8.020 g, 28.813 mmol, 99%).

¹H NMR (400 MHz, CDCl₃): δ 3.31 (s, 1H), 5.46 (s, 1H), 7.05–7.12 (m, 6H), 7.41–7.43 (m, 3H), 7.78–7.80 (m, 3H). ¹³C NMR (400 MHz, CDCl₃): δ 52.9, 53.2, 78.4, 80.5, 122.3, 123.4, 125.2, 125.7, 143.8, 144.3, in agreement with literature.³⁰

9-(3-Hydroxyprop-1-ynyl)-10-(trimethylsilylethynyl)triptycene (16). To a solution of **7** (3.260 g, 8.704 mmol) in THF (60 mL) at -78 °C was dropwise added *n*-BuLi in hexane (1.6 M, 6.53 mL, 10.445 mmol). A dense white precipitate formed immediately. The white suspension was stirred for 60 min at -78 °C. Subsequently, dry solid paraformaldehyde (784 mg, 26.112 mmol) was added, and the suspension was stirred for 90 min at -78 °C. Cooling was discontinued, the reaction mixture was slowly warmed to room temperature and stirred for 3 h. The reaction was quenched with saturated aqueous NH₄Cl (15 mL), and the solution was stirred for 30 min. The reaction mixture was diluted with ether (150 mL) and washed with saturated aqueous NH₄Cl (3 × 40 mL), and the clear yellowish organic phase was dried over MgSO₄. Volatiles were removed under reduced pressure. Column chromatography on silica gel (CH₂Cl₂) gave **16** (2.560 g, 6.328 mmol, 73%) as a white crystalline solid.

Mp 299.0–300.4 °C. ¹H NMR (400 MHz, CDCl₃): δ 0.50 (s, 9H), 2.02 (br s, 1H), 4.82 (s, 2H), 7.11–7.14 (m, 6H), 7.74–7.77 (m, 6H). ¹³C NMR (100 MHz, CDCl₃): δ 0.3, 51.6, 52.3, 53.0, 80.0, 91.3, 98.2, 99.5, 122.1, 122.3, 125.7, 125.8, 143.2. IR (KBr): 3572, 3561, 3071, 3063, 3049, 3035, 3014, 2954, 2897, 2860, 2184, 2167, 1608, 1596, 1455, 1447, 1408, 1380, 1342, 1338, 1306, 1256, 1246, 1232, 1202, 1173, 1165, 1157, 1155, 1139, 1116, 1057, 1030, 1021, 978, 963, 953, 908, 863, 841, 771, 756, 699, 687, 660, 653, 640, 609, 579, 554, 551, 494, 483, 444 cm⁻¹. MS, *m/z* (%): 427.2 (M + Na). HRMS, (ESI+) for (C₂₈H₂₄O₂Si + Na⁺): calcd 427.14886, found 427.14878. Anal. calcd for C₂₈H₂₄O₂Si: C, 83.12; H, 5.98. Found: C, 82.96; H, 5.98.

9-(3-Oxoprop-1-ynyl)-10-(trimethylsilylethynyl)triptycene (17). To a solution of DMSO (2.70 mL, 38.066 mmol) in CH₂Cl₂ (15 mL) was added (COCl)₂ (2.30 mL, 27.190 mmol) at -78 °C. The reaction mixture turned slightly yellow. After 30 min at this temperature, **16** (2.200 g, 5.438 mmol) in CH₂Cl₂ (40 mL) was slowly introduced, and the milky solution was stirred 2 h at -78 °C. Then triethylamine (7.58 mL, 54.380 mmol) was added. The mixture was stirred for 30 min and then warmed to room temperature and stirred for 90 min. A white precipitate partially dissolved, leaving a yellow suspension. Volatiles were removed under reduced pressure, and the yellow solid was sorbed on silica gel (8 g). Column chromatography on silica gel (hexane/CH₂Cl₂, 1:1) yielded **17** as a white crystalline solid (1.828 g, 4.541 mmol, 84%).

Mp 259.2–260.8 °C. ¹H NMR (400 MHz, CDCl₃): δ 0.50 (s, 9H), 7.12–7.18 (m, 6H), 7.68–7.70 (m, 3H), 7.77–7.79 (m, 3H), 9.75 (s, 1H). ¹³C NMR (100 MHz, CDCl₃): δ 0.3, 52.3, 53.1, 90.4, 91.5, 98.6, 99.0, 121.8, 122.7, 125.9, 126.2, 141.8, 143.0, 176.3. IR (KBr): 3071,

3063, 3049, 3036, 3015, 2953, 2897, 2858, 2254, 2235, 2216, 2184, 2166, 1677, 1608, 1596, 1459, 1454, 1445, 1409, 1387, 1306, 1257, 1247, 1230, 1167, 1154, 1138, 1056, 1031, 930, 866, 841, 764, 751, 700, 693, 668, 640, 605, 492, 484 cm⁻¹. MS, *m/z* (%): 402.1 (100, M), 385.1 (31, M - CH₃), 374.2 (28, M - CHO), 359.1 (11), 343.1 (16), 329.1 (24, M - TMS), 313.1 (41), 300.1 (29), 289.1 (16), 276.1 (27), 252.1 (8), 73.0 (45, TMS). HRMS, (EI) for (C₂₈H₂₂O₂Si⁺): calcd 402.1440, found 402.1447. Anal. calcd for C₂₈H₂₂O₂Si: C, 83.54; H, 5.51. Found: C, 83.89; H, 5.46.

9-(4,4-Dibromobut-3-en-1-ynyl)-10-(trimethylsilylethynyl)-tritycene (18). A flame-dried and argon filled Schlenk flask was charged with PPh₃ (3.870 g, 14.754 mmol) and CBr₄ (2.224 g, 6.707 mmol). After three successive vacuum/argon cycles, the mixture was cooled to 0 °C using ice bath, dry and degassed CH₂Cl₂ was added (15 mL), and the orange reaction mixture was stirred 40 min at 0 °C. Then a solution of 17 (1.800 g, 4.471 mmol) in dry CH₂Cl₂ (30 mL) was added dropwise, and the brown reaction mixture was stirred 10 min at 0 °C. Cooling was discontinued, and the brown solution was stirred for 3 h at room temperature. Silica gel (15 g) was added directly to the reaction mixture, and all volatiles were removed under reduced pressure. Column chromatography on silica gel (hexane/CH₂Cl₂, 1:1) provided 18 as a white crystalline solid (1.896 g, 3.396 mmol, 76%).

Mp 272.2–273.9 °C. ¹H NMR (400 MHz, CDCl₃): δ 0.49 (s, 9H), 7.10 (s, 1H), 7.11–7.15 (m, 6H), 7.74–7.77 (m, 6H). ¹³C NMR (100 MHz, CDCl₃): δ 0.3, 53.1, 53.2, 89.2, 91.9, 98.3, 99.4, 103.5, 119.3, 122.2, 122.4, 125.7, 125.8, 143.0, 143.2. IR (KBr): 3069, 3033, 3015, 2956, 2223, 2185, 2173, 1609, 1457, 1453, 1444, 1426, 1307, 1261, 1251, 1232, 1156, 1144, 1125, 1057, 1032, 974, 954, 861, 842, 821, 751, 744, 702, 689, 661, 639, 612, 580, 492 cm⁻¹. MS, *m/z* (%): 558.0 (100, M, center of isotope cluster), 543.0 (11, M - CH₃, center of isotope cluster), 479.1 (20, M - Br, center of isotope cluster), 459.9 (17, center of isotope cluster), 398.2 (38), 383.1 (19), 367.1 (18), 348.1 (23), 337.1 (22), 325.1 (48), 300.1 (28), 276.1 (13), 263.1 (6), 252.1 (10), 73.0 (51, TMS). HRMS, (EI) for (C₂₉H₂₂Br₂Si⁺): calcd 555.9858, found 555.9874. Anal. calcd for C₂₉H₂₂Br₂Si: C, 62.38; H, 3.97. Found: C, 62.47; H, 3.97.

9-(Buta-1,3-diyne)tritycene (19). The solution of *n*-BuLi in hexane (2.5 M, 5.19 mL, 12.981 mmol) was added dropwise to a solution of 22 (2.000 g, 4.327 mmol) in THF (50 mL) cooled to -78 °C. The brownish reaction mixture was stirred at -78 °C for 3 h. A dense white precipitate was formed. Subsequently, concentrated aqueous NH₄Cl (10 mL) was added, and cooling was discontinued. The yellowish reaction mixture was diluted with ether (150 mL) and washed with saturated aqueous NH₄Cl (2 × 40 mL). The clear yellowish organic phase was dried over MgSO₄, and volatiles were removed under reduced pressure. Column chromatography on silica gel (hexane/CH₂Cl₂, 5:1) gave 19 as a white crystalline solid (1.152 g, 3.810 mmol, 88%).

Mp 190.4–191.2 °C. ¹H NMR (400 MHz, CDCl₃): δ 2.45 (s, 1H), 5.48 (s, 1H), 7.08–7.15 (m, 6H), 7.44–7.46 (m, 3H), 7.78–7.80 (m, 3H). ¹³C NMR (100 MHz, CDCl₃): δ 53.1, 53.3, 67.8, 68.3, 71.9, 76.0, 122.3, 123.5, 125.3, 125.9, 143.6, 144.1. IR (KBr): 3283, 3272, 3069, 3059, 3037, 3016, 3005, 2964, 2953, 2932, 2245, 1609, 1595, 1582, 1457, 1323, 1303, 1291, 1276, 1256, 1194, 1170, 1153, 1145, 1138, 1092, 1026, 974, 948, 903, 868, 861, 833, 760, 749, 691, 642, 625, 608, 529, 526, 488, 478 cm⁻¹. MS, *m/z* (%): 303.1 (100, M + H). HRMS, (APCI) for (C₂₄H₁₄ + H⁺): calcd 303.11683, found 303.11692. Anal. calcd for C₂₄H₁₄: C, 95.33; H, 4.67. Found: C, 95.35; H, 4.64.

9-(3-Hydroxyprop-1-ynyl)tritycene (20). To a solution of 15 (3.340 g, 12.000 mmol) in THF (100 mL) at -78 °C was dropwise added *n*-BuLi in hexane (2.5 M, 5.80 mL, 14.500 mmol). A dense white precipitate formed immediately. The white suspension was stirred for 60 min at -78 °C. Subsequently, dry solid paraformaldehyde (1.306 g, 43.500 mmol) was added, and suspension was stirred for 60 min at -78 °C. Cooling was discontinued, and the reaction mixture was slowly warmed to room temperature and stirred for 16 h. The solids dissolved, leaving a clear yellow solution. The reaction was quenched with saturated aqueous NH₄Cl (30 mL), and solution was stirred for 30 min. The reaction mixture was diluted with ether (150 mL) and washed with saturated aqueous NH₄Cl (3 × 30 mL), and a

clear yellowish organic phase was dried over MgSO₄. Volatiles were removed under reduced pressure. Column chromatography on silica gel (CH₂Cl₂) gave 20 (2.559 g, 8.298 mmol, 69%) as a white crystalline solid.

Mp 282.5–283.7 °C. ¹H NMR (500 MHz, CDCl₃): δ 1.95 (s, 1H), 4.81 (s, 2H), 5.44 (s, 1H), 7.03–7.09 (m, 6H), 7.40–7.41 (m, 3H), 7.72–7.74 (m, 3H). ¹³C NMR (125 MHz, CDCl₃): δ 51.6, 53.0, 53.2, 80.3, 90.9, 122.3, 123.4, 125.1, 125.7, 144.1, 144.3. IR (KBr): 3581, 3551, 3401, 3300, 3093, 3066, 3036, 3015, 2957, 2943, 2918, 2867, 2253, 1607, 1580, 1456, 1439, 1382, 1372, 1357, 1346, 1301, 1290, 1255, 1211, 1193, 1171, 1151, 1144, 1134, 1088, 1024, 1018, 982, 969, 941, 919, 859, 859, 833, 765, 755, 694, 641, 608, 578, 522, 482 cm⁻¹. MS, *m/z* (%): 331.2 (100, M + Na). HRMS, (ESI+) for (C₂₃H₁₆O + Na⁺): calcd 331.10934, found 331.10947. Anal. calcd for C₂₃H₁₆O: C, 89.58; H, 5.23. Found: C, 89.69; H, 5.14.

9-(3-Oxoprop-1-ynyl)tritycene (21).³¹ To a solution/suspension of 20 (2.300 g, 7.459 mmol) in dry CH₂Cl₂ (70 mL) was added Dess–Martin periodinane (DMP, 3.796 g, 8.951 mmol) at room temperature. The solution turned yellow immediately and was stirred for 2 h. The suspension dissolved, leaving a clear yellowish solution. Solutions of saturated aqueous Na₂S₂O₃ (30 mL) and NaHCO₃ (30 mL) were added, and the mixture was stirred for 30 min. CH₂Cl₂ (50 mL) was added. The aqueous phase was removed, and the clear yellowish organic phase was washed with saturated aqueous solution of Na₂S₂O₃ and NaHCO₃ (1:1, 2 × 40 mL) and dried over MgSO₄. Solvent was removed under reduced pressure, and a solid yellow residue was sorbed on silica gel (6 g). Column chromatography on silica gel (CH₂Cl₂) afforded 21 as a white crystalline solid (2.186 g, 7.135 mmol, 96%).

Mp 273.9–274.8 °C. ¹H NMR (400 MHz, CDCl₃): δ 5.49 (s, 1H), 7.08–7.13 (m, 6H), 7.44–7.46 (m, 3H), 7.70–7.72 (m, 3H), 9.76 (s, 1H). ¹³C NMR (100 MHz, CDCl₃): δ 53.0, 53.2, 90.9, 91.3, 122.0, 123.7, 125.4, 126.1, 142.7, 144.0, 176.4. IR (KBr): 3068, 3047, 3016, 3006, 2955, 2859, 2743, 2221, 1677, 1607, 1580, 1500, 1457, 1437, 1388, 1302, 1293, 1253, 1192, 1172, 1152, 1143, 1093, 1087, 1026, 978, 942, 914, 869, 859, 834, 751, 704, 671, 641, 635, 607, 525, 482 cm⁻¹. MS, *m/z* (%): 307.1 (100, M + H). HRMS, (APCI) for (C₂₃H₁₄O + H⁺): calcd 307.11174, found 307.11174. Anal. calcd for C₂₃H₁₄O: C, 90.17; H, 4.61. Found: C, 89.98; H, 4.58.

9-(4,4-Dibromobut-3-en-1-ynyl)tritycene (22). A flame-dried and argon filled Schlenk flask was charged with PPh₃ (5.650 g, 24.542 mmol) and CBr₄ (3.247 g, 9.792 mmol). After three successive vacuum/argon cycles, the mixture was cooled to 0 °C. Dry and degassed CH₂Cl₂ (30 mL) was added, and the orange reaction mixture was stirred 40 min at 0 °C. A solution of 21 (2.000 g, 6.528 mmol) in dry CH₂Cl₂ (30 mL) was added dropwise, and the brown reaction mixture was stirred 10 min at 0 °C. Cooling was discontinued, and the brown solution was stirred for 2 h at room temperature. Silica gel (20 g) was added directly to the reaction mixture, and all volatiles were removed under reduced pressure. Column chromatography on silica gel (hexane/CH₂Cl₂, 1:1) provided 22 as a white crystalline solid (2.524 g, 5.461 mmol, 84%).

Mp 240.8–242.0 °C. ¹H NMR (400 MHz, CDCl₃): δ 5.47 (s, 1H), 7.05–7.12 (m, 6H), 7.11 (s, 1H), 7.42–7.44 (m, 3H), 7.78–7.80 (m, 3H). ¹³C NMR (100 MHz, CDCl₃): δ 53.3, 53.9, 88.9, 92.4, 103.3, 119.4, 122.4, 123.5, 125.2, 125.8, 143.8, 144.3. IR (KBr): 3070, 3045, 3037, 3016, 2957, 2959, 2228, 1634, 1607, 1594, 1576, 1571, 1456, 1391, 1304, 1289, 1267, 1194, 1184, 1171, 1155, 1142, 1026, 971, 942, 914, 868, 826, 819, 748, 744, 695, 641, 609, 578, 530, 521, 488, 481, 464 cm⁻¹. MS, *m/z* (%): 463.0 (100, M + H). HRMS, (APCI) for (C₂₄H₁₄Br₂ + H⁺): calcd 460.95350, found 460.95349. Anal. calcd for C₂₄H₁₄Br₂: C, 62.37; H, 3.05. Found: C, 61.98; H, 3.06.

2,3-Dichloro-1-iodo-4-methylbenzene (23). To a solution of 2,3-dichlorotoluene (26) (1.50 g, 9.315 mmol) in THF (20 mL) was slowly added a solution of *n*-BuLi in hexane (2.5 M, 4.47 mL, 11.178 mmol) at -78 °C. The slightly yellowish reaction mixture was stirred at -78 °C for 90 min, while a dense white solid precipitated. Subsequently a solution of freshly sublimed I₂ (3.173 g, 12.500 mmol) in THF (20 mL) was added dropwise, and the dark red reaction mixture was stirred for 10 min at -78 °C. Cooling was discontinued,

and the reaction mixture was allowed to warm to 0 °C. Excess iodine was removed by addition of 50% aqueous Na₂SO₃ (20 mL). The reaction mixture was diluted with ether (150 mL) and washed with 50% aqueous Na₂SO₃ (3 × 50 mL). The colorless organic phase was dried over MgSO₄, and solvents were removed under reduced pressure. The flask with a yellowish oily residue was connected to Kugelrohr distillation apparatus, and the mixture was distilled under reduced pressure (550 mTorr). The oven temperature was slowly raised to 110 °C. In the receiving flask, the starting material was collected first as a colorless oil. The temperature in the oven was then increased to 130 °C and **23** distilled (130 °C, 550 mTorr) as a colorless oil, which slowly solidified (994 mg, 3.464 mmol, 37%).

Mp 38.9–40.7 °C. ¹H NMR (400 MHz, CDCl₃): δ 2.38 (s, 3H), 6.87 (dd, *J*₁ = 0.53 Hz, *J*₂ = 8.14 Hz, 1H), 7.65 (d, *J* = 8.11 Hz, 1H). ¹³C NMR (100 MHz, CDCl₃): δ 21.2, 95.2, 129.9, 132.7, 136.8, 137.4, 138.5. IR (KBr): 3059, 3045, 1569, 1553, 1446, 1432, 1400, 1380, 1358, 1238, 1208, 1170, 1153, 1138, 1082, 1065, 1034, 1006, 870, 804, 770, 752, 717, 692, 627 cm⁻¹. MS, *m/z* (%): 286.9 (100, M, center of isotope cluster), 200.0 (14, M – Cl, center of isotope cluster), 188.0 (41, center of isotope cluster), 161.0 (82, center of isotope cluster). HRMS, (CI) for (C₇H₅Cl₂I + H⁺): calcd 286.8891, found 286.8901. Anal. calcd for C₇H₅Cl₂I: C, 29.30; H, 1.76. Found: C, 29.67; H, 1.76.

2,3-Dichloro-1-iodo-4-methyl-(d₃)-benzene (24). The procedure for **23** was followed, starting with a solution of **27** (1.50 g, 9.144 mmol) in THF (20 mL) and a solution of *n*-BuLi in hexane (2.5 M, 4.39 mL, 10.972 mmol) at –78 °C. The yield of **24** was 1.046 g (3.608 mmol, 39%).

Mp 39.1–40.4 °C. ¹H NMR (400 MHz, CDCl₃): δ 6.86 (d, *J* = 8.12 Hz, 1H), 7.65 (d, *J* = 8.11 Hz, 1H). ²H NMR (76 MHz, CHCl₃): δ 2.36 (s, 3D). ¹³C NMR (100 MHz, CDCl₃): δ 20.4 (sep, *J*_{C,D} = 19.8 Hz), 95.2, 129.9, 132.7, 136.7, 137.4, 138.4. IR (KBr): 3109, 3077, 3040, 2989, 2956, 2927, 2869, 2858, 2236, 2213, 2165, 2134, 2103, 2056, 1893, 1569, 1535, 1468, 1434, 1400, 1354, 1254, 1208, 1168, 1142, 1106, 1082, 1038, 962, 949, 873, 863, 787, 756, 685, 605, 523 cm⁻¹. MS, *m/z* (%): 288.9 (75, M + H, center of isotope cluster), 253.9 (10), 191.0 (36), 163.0 (100, M – I, center of isotope cluster), 128.0 (12), 92.1 (11), 65.0 (8). HRMS, (CI) for (C₇H₂²H₃Cl₂I + H⁺): calcd 289.9080, found 289.9073. Anal. calcd for C₇H₂²H₃Cl₂I: C, 29.00; H, 1.75. Found: C, 29.27; H, 1.83.

2,3-Dichlorotoluene (26).^{51,52} To a solution of 1,2-dichlorobenzene (**25**) (5.63 mL, 50.000 mmol) in THF (80 mL) was slowly added (1.50 mL/min) a solution of *n*-BuLi in hexane (1.6 M, 37.50 mL, 60.000 mmol) at –78 °C. The slightly yellowish reaction mixture was stirred at –78 °C for 60 min, while a dense white solid precipitated. Subsequently CH₃I (3.86 mL, 62.000 mmol) was added dropwise, and the reaction mixture was stirred for 30 min at –78 °C. Cooling was discontinued, and the reaction mixture was allowed to warm to room temperature. The precipitate dissolved, leaving a clear yellowish solution. The reaction mixture was diluted with ether (150 mL), washed with water (2 × 50 mL), concentrated aqueous NH₄Cl (2 × 50 mL), and dried over MgSO₄. Solvents were carefully distilled off at atmospheric pressure and an oil bath temperature of 110 °C using a Vigreux column. Distillation of yellowish oily residue at reduced pressure (water aspirator: 20 Torr, temperature of oil bath: 120 °C) provided **26** (88–90 °C, 20 Torr) as a colorless liquid (4.094 g, 25.424 mmol, 51%).

¹H NMR (400 MHz, CDCl₃): δ 2.42 (s, 3H), 7.08 (dd, *J*₁ = 7.49 Hz, *J*₂ = 7.92 Hz, 1H), 7.13 (dd, *J*₁ = 1.02 Hz, *J*₂ = 7.48 Hz, 1H), 7.30 (dd, *J*₁ = 1.39 Hz, *J*₂ = 7.78 Hz, 1H). ¹³C NMR (100 MHz, CDCl₃): δ 21.1, 126.8, 127.9, 128.9, 132.6, 132.8, 138.4.

1,2-Dichloro-3-methyl-(d₃)-benzene (27). The procedure for **26** was followed, starting with a solution of **25** (9.00 mL, 80.000 mmol) in THF (100 mL), a solution of *n*-BuLi in hexane (2.5 M, 38.40 mL, 96.000 mmol), and CD₃I (6.54 mL, 105.000 mmol). The yield of **27** (89–91 °C, 20 Torr) was 7.445 g (45.383 mmol, 57%).

¹H NMR (400 MHz, CDCl₃): δ 7.09 (dd, *J*₁ = 7.54 Hz, *J*₂ = 7.83 Hz, 1H), 7.13 (dd, *J*₁ = 1.83 Hz, *J*₂ = 7.60 Hz, 1H), 7.30 (dd, *J*₁ = 1.83 Hz, *J*₂ = 7.75 Hz, 1H). ²H NMR (76 MHz, CHCl₃): δ 2.40 (s, 3D). ¹³C NMR (100 MHz, CDCl₃): δ 20.3 (sep, *J*_{C,D} = 19.8 Hz), 126.8, 127.9, 128.9, 132.6, 132.8, 138.3. IR (KBr): 3067, 3056, 3013, 2996,

2958, 2929, 2236, 2213, 2118, 2060, 1586, 1577, 1563, 1460, 1449, 1434, 1417, 1273, 1189, 1175, 1160, 1152, 1110, 1066, 1038, 911, 856, 793, 758, 736, 686, 549 cm⁻¹. MS, *m/z* (%): 163.0 (64, M, center of isotope cluster), 128.0 (100, M – Cl, center of isotope cluster), 91.1 (14). HRMS, (EI) for (C₇H₃²H₃Cl₂⁺): calcd 163.0035, found 163.0039. Anal. calcd for C₇H₃²H₃Cl₂: C, 51.25; H, 3.70. Found: C, 51.55; H, 3.80.

3-Iodo-6-methylpyridazine (28).³² A previously published procedure³² was adapted as follows: A solution of 3-chloro-6-methylpyridazine (500 mg, 3.889 mmol) and NaI (816 mg, 5.445 mmol) in 57% aqueous HI (7 mL) was stirred 30 min at 40 °C, 16 h at 70 °C, and finally 3 h at 100 °C. A dense yellow precipitate was formed. The reaction mixture was cooled to room temperature and then carefully poured into the ice-cold 70% aqueous NaOH (60 mL). The aqueous phase was extracted with CH₂Cl₂ (3 × 25 mL), and a slightly yellowish combined organic phases were dried over MgSO₄. Solvent was removed under reduced pressure and column chromatography on silica gel (hexane/ethyl-acetate, 2:3) yielded **28** as a white crystalline solid (815 mg, 3.704 mmol, 95%).

Mp 92.3–93.9 °C. ¹H NMR (400 MHz, CDCl₃): δ 2.60 (s, 3H), 7.01 (d, *J* = 8.67 Hz, 1H), 7.71 (d, *J* = 8.66 Hz, 1H). (ref 32) ¹³C NMR (100 MHz, CDCl₃): δ 21.7, 122.4, 128.1, 136.8, 159.4. IR (KBr): 3129, 3098, 3071, 3017, 2956, 2921, 1566, 1531, 1482, 1415, 1401, 1377, 1321, 1240, 1203, 1160, 1110, 1047, 1017, 978, 842, 833, 809, 781, 636, 604, 488 cm⁻¹. MS, *m/z* (%): 243.0 (11, M + Na), 221.0 (100, M + H). HRMS, (ESI⁺) for (C₅H₅IN₂ + H⁺): calcd 220.95702, found 220.95696. Anal. calcd for C₅H₅IN₂: C, 27.30; H, 2.29; N, 12.73. Found: C, 27.45; H, 2.17; N, 12.43.

General Procedure for Sonogashira Coupling between Rotators and Triptycene Units (GP 1). A flame-dried Schlenk flask was charged with the alkyne **7** (1 equiv), rotator **23**, **24**, **28**, or **29** (1.2 equiv), Pd(PPh₃)₄ (4 mol %), and CuI (3 mol %). After three successive vacuum/argon cycles, dry and degassed THF (5 mL) and triethylamine (4 mL) were added from a syringe. The slightly yellowish solution was stirred for 18 h at room temperature. A dense white solid precipitated. A crude reaction mixture was diluted with CH₂Cl₂ (80 mL), washed with saturated aqueous NH₄Cl (2 × 20 mL), and dried over MgSO₄. Volatiles were removed under reduced pressure. Column chromatography on silica gel gave silyl derivatives **30–33** as white crystalline solids.

9-(2,3-Dichlorophenylbuta-1,3-dienyl)-10-(trimethylsilylethynyl)triptycene (30). According to GP 1, **30** was prepared from **29** (205 mg, 0.752 mmol), **7** (250 mg, 0.627 mmol), Pd(PPh₃)₄ (29 mg, 0.025 mmol), and CuI (4 mg, 0.019 mmol) in mixture of THF (5 mL) and triethylamine (4 mL). Column chromatography on silica gel (hexane/CH₂Cl₂, 4:1) yielded **30** as a white crystalline solid (316 mg, 0.581 mmol, 93%).

Mp 259.0–260.2 °C. ¹H NMR (400 MHz, CDCl₃): δ 0.50 (s, 9H), 7.14–7.16 (m, 6H), 7.23 (t, *J* = 7.93 Hz, 1H), 7.52 (dd, *J*₁ = 1.44 Hz, *J*₂ = 8.10 Hz, 1H), 7.62 (dd, *J*₁ = 1.22 Hz, *J*₂ = 7.75 Hz, 1H), 7.75–7.80 (m, 6H). ¹³C NMR (100 MHz, CDCl₃): δ 0.3, 53.0, 53.1, 74.3, 76.4, 79.0, 79.7, 98.3, 99.3, 122.1, 122.4, 123.8, 125.8, 126.0, 127.2, 131.3, 132.7, 133.6, 135.5, 142.9, 143.1. IR (KBr): 3068, 3047, 2954, 2173, 1606, 1579, 1554, 1453, 1445, 1413, 1346, 1337, 1295, 1247, 1223, 1192, 1158, 1124, 1098, 1055, 1049, 1032, 977, 960, 945, 896, 856, 842, 792, 781, 756, 753, 727, 703, 658, 639, 610, 587, 566 cm⁻¹. MS, *m/z* (%): 543.1 (100, M + H), 471.1 (20, M – TMS). HRMS, (APCI) for (C₃₅H₂₄Cl₂Si + H⁺): calcd 543.10971, found 543.10929. Anal. calcd for C₃₅H₂₄Cl₂Si: C, 77.34; H, 4.45. Found: C, 77.65; H, 4.33.

9-(2,3-Dichloro-4-methylphenylbuta-1,3-dienyl)-10-(trimethylsilylethynyl)triptycene (31). According to GP 1, **31** was prepared from **23** (130 mg, 0.452 mmol), **7** (150 mg, 0.376 mmol), Pd(PPh₃)₄ (17 mg, 0.015 mmol), and CuI (2 mg, 0.011 mmol) in mixture of THF (5 mL) and triethylamine (4 mL). Column chromatography on silica gel (hexane/CH₂Cl₂, 4:1) yielded **31** as a white crystalline solid (191 mg, 0.343 mmol, 91%).

Mp 269.1–270.3 °C. ¹H NMR (400 MHz, CDCl₃): δ 0.49 (s, 9H), 2.48 (s, 3H), 7.13–7.15 (m, 6H), 7.17 (dd, *J*₁ = 0.54 Hz, *J*₂ = 7.86 Hz, 1H), 7.52 (d, *J* = 7.91 Hz, 1H), 7.74–7.79 (m, 6H). ¹³C NMR (100 MHz, CDCl₃): δ 0.3, 21.6, 53.0, 53.1, 74.7, 76.5, 78.2, 79.2, 98.3, 99.3,

121.0, 122.2, 122.4, 125.8, 125.9, 128.6, 131.8, 133.6, 135.7, 140.0, 143.0, 143.1. IR (KBr): 3070, 3049, 3034, 2958, 2919, 2183, 2175, 1606, 1459, 1453, 1445, 1411, 1370, 1341, 1296, 1247, 1221, 1167, 1153, 1098, 1056, 1033, 1014, 952, 871, 845, 820, 783, 758, 753, 703, 694, 639, 608 cm^{-1} . MS, m/z (%): 579.0 (100, M + Na). HRMS, (ESI+) for ($\text{C}_{36}\text{H}_{26}\text{Cl}_2\text{Si} + \text{Na}^+$): calcd 579.10730, found 579.10734. Anal. calcd for $\text{C}_{36}\text{H}_{26}\text{Cl}_2\text{Si}$: C, 77.55; H, 4.70. Found: C, 77.35; H, 4.60.

9-[2,3-Dichloro-4-methyl(d_3)phenylbuta-1,3-diyne]-10-(trimethylsilylethynyl)triptycene (32). According to GP 1, 32 was prepared from 24 (218 mg, 0.752 mmol), 7 (250 mg, 0.627 mmol), Pd(PPh₃)₄ (29 mg, 0.025 mmol), and CuI (4 mg, 0.019 mmol) in mixture of THF (5 mL) and triethylamine (4 mL). Column chromatography on silica gel (hexane/ CH_2Cl_2 , 4:1) yielded 32 as a white crystalline solid (346 mg, 0.617 mmol, 98%).

Mp 271.8–273.2 °C. ¹H NMR (400 MHz, CDCl_3): δ 0.50 (s, 9H), 7.13–7.17 (m, 6H), 7.17 (d, J = 8.09 Hz, 1H), 7.52 (d, J = 7.92 Hz, 1H), 7.76–7.81 (m, 6H). ²H NMR (76 MHz, CHCl_3): δ 2.46 (s, 3D). ¹³C NMR (100 MHz, CDCl_3): δ 0.3, 53.0, 53.1, 74.7, 76.6, 78.2, 79.2, 98.3, 99.3, 121.0, 122.2, 122.4, 125.8, 125.9, 128.6, 131.8, 133.6, 135.7, 139.9, 143.0, 143.1 (Carbon signal of CD_3 group was not detected due to strong ¹³C–²H coupling). IR (KBr): 3070, 3049, 3035, 2958, 2898, 2236, 2215, 2177, 2155, 2130, 1949, 1942, 1919, 1911, 1606, 1581, 1458, 1453, 1445, 1423, 1411, 1372, 1341, 1296, 1246, 1220, 1167, 1153, 1140, 1102, 1059, 1052, 1033, 978, 950, 923, 880, 845, 801, 777, 757, 753, 747, 698, 691, 665, 650, 639, 607, 571, 490, 476, 441 cm^{-1} . MS, m/z (%): 582.2 (81, M + Na), 560.3 (100, M + H). HRMS, (ESI+) for ($\text{C}_{36}^1\text{H}_{23}^2\text{H}_3\text{Cl}_2\text{Si} + \text{H}^+$): calcd 560.14419, found 560.14437. Anal. calcd for $\text{C}_{36}^1\text{H}_{23}^2\text{H}_3\text{Cl}_2\text{Si}$: C, 77.13; H, 4.68. Found: C, 77.16; H, 4.61.

9-((6-Methylpyridazin-3-yl)buta-1,3-diyne)-10-(trimethylsilylethynyl)triptycene (33). According to GP 1, 33 was prepared from 28 (166 mg, 0.752 mmol), 7 (250 mg, 0.627 mmol), Pd(PPh₃)₄ (29 mg, 0.025 mmol), and CuI (4 mg, 0.019 mmol) in mixture of THF (5 mL) and triethylamine (4 mL). Column chromatography on silica gel (hexane/acetone, 3:1, then hexane/acetone, 1:1) yielded 33 as a white crystalline solid (268 mg, 0.546 mmol, 87%).

Mp > 180 °C (dec.). ¹H NMR (400 MHz, CDCl_3): δ 0.49 (s, 9H), 2.80 (s, 3H), 7.13–7.15 (m, 6H), 7.31 (d, J = 8.57 Hz, 1H), 7.61 (d, J = 8.56 Hz, 1H), 7.74–7.77 (m, 6H). ¹³C NMR (100 MHz, CDCl_3): δ 0.3, 22.5, 52.95, 52.97, 74.4, 76.0, 77.2, 80.1, 98.4, 99.1, 122.0, 122.4, 125.9, 126.0, 126.1, 130.3, 142.7, 143.0, 145.0, 159.0. IR (KBr): 3070, 3044, 3015, 2958, 2921, 2899, 2252, 2239, 2184, 2171, 1607, 1592, 1538, 1459, 1453, 1445, 1414, 1314, 1305, 1251, 1237, 1215, 1168, 1149, 1140, 1084, 1055, 1032, 1003, 953, 945, 863, 859, 843, 816, 769, 763, 752, 695, 651, 639, 610 cm^{-1} . MS, m/z (%): 513.4 (19, M + Na), 491.4 (100, M + H). HRMS, (ESI+) for ($\text{C}_{34}\text{H}_{26}\text{N}_2\text{Si} + \text{H}^+$): calcd 491.19380, found 491.19345. Anal. calcd for $\text{C}_{34}\text{H}_{26}\text{N}_2\text{Si}$: C, 83.23; H, 5.34; N, 5.71. Found: C, 83.42; H, 5.19; N, 5.45.

General Procedure for TMS Removal (GP 2). To a stirred solution of silyl derivatives 30–33 (1 equiv) in wet THF (8 mL), a solution of TBAF in THF (1.0 M, 1.2 equiv) was added at room temperature. The reddish reaction mixture was stirred for 30 min, diluted with CH_2Cl_2 (60 mL), washed with water (2 × 20 mL), and the clear yellowish organic phase was dried over MgSO_4 . Solvents were removed under reduced pressure and a column chromatography on silica gel gave alkynes 34–37 as white crystalline solids.

9-(2,3-Dichlorophenylbuta-1,3-diyne)-10-ethynyltriptycene (34). According to GP 2, 34 was synthesized from 30 (290 mg, 0.534 mmol) and a mixture of TBAF in THF (1.0 M, 641 μL , 0.641 mmol) with THF (8 mL). Column chromatography on silica gel (hexane/ CH_2Cl_2 , 3:1) gave 34 as a white crystalline solid (248 mg, 0.526 mmol, 99%).

Mp 294.5–295.8 °C. ¹H NMR (400 MHz, CDCl_3): δ 3.31 (s, 1H), 7.12–7.15 (m, 6H), 7.25 (t, J = 7.89 Hz, 1H), 7.53 (dd, J_1 = 1.45 Hz, J_2 = 8.09 Hz, 1H), 7.62 (dd, J_1 = 1.45 Hz, J_2 = 7.74 Hz, 1H), 7.76–7.78 (m, 6H). ¹³C NMR (100 MHz, CDCl_3): δ 52.2, 53.1, 74.4, 76.4, 77.8, 79.0, 79.6, 81.0, 122.2, 122.3, 123.8, 125.9, 126.0, 127.2, 131.3, 132.8, 133.6, 135.5, 142.8, 142.9. IR (KBr): 3268, 3253, 3068, 2123, 1606,

1597, 1577, 1550, 1458, 1453, 1445, 1423, 1412, 1407, 1346, 1339, 1324, 1305, 1294, 1262, 1244, 1220, 1156, 1150, 1122, 1094, 1080, 1047, 1041, 1032, 976, 946, 922, 907, 875, 864, 784, 759, 754, 705, 677, 666, 639 cm^{-1} . MS, m/z (%): 471.1 (100, M + H, center of isotope cluster). HRMS, (APCI) for ($\text{C}_{32}\text{H}_{16}\text{Cl}_2 + \text{H}^+$): calcd 471.07018, found 471.06977. Anal. calcd for $\text{C}_{32}\text{H}_{16}\text{Cl}_2$: C, 81.54; H, 3.42. Found: C, 81.85; H, 3.43.

9-(2,3-Dichloro-4-methylphenylbuta-1,3-diyne)-10-ethynyltriptycene (35). According to GP 2, 35 was synthesized from 31 (190 mg, 0.341 mmol) and a mixture of TBAF in THF (1.0 M, 409 μL , 0.409 mmol) with THF (8 mL). Column chromatography on silica gel (hexane/ CH_2Cl_2 , 3:1) gave 35 as a white crystalline solid (160 mg, 0.330 mmol, 97%).

Mp 298.4–299.7 °C. ¹H NMR (400 MHz, $\text{THF}-d_6$): δ 2.47 (s, 3H), 3.98 (s, 1H), 7.11–7.13 (m, 6H), 7.32 (dd, J_1 = 0.59 Hz, J_2 = 7.96 Hz, 1H), 7.63 (d, J = 7.88 Hz, 1H), 7.72–7.74 (m, 3H), 7.75–7.77 (m, 3H). ¹³C NMR (100 MHz, $\text{THF}-d_6$): δ 21.5, 53.3, 54.2, 75.6, 77.5, 78.4, 78.7, 80.1, 83.3, 121.8, 122.8, 123.2, 126.8, 126.9, 130.1, 133.2, 134.3, 136.2, 141.5, 144.0, 144.1. IR (KBr): 3294, 3282, 3069, 3046, 3032, 2161, 1607, 1454, 1444, 1411, 1368, 1342, 1305, 1246, 1237, 1217, 1167, 1158, 1096, 1033, 1017, 977, 950, 874, 818, 781, 752, 747, 676, 668, 657, 653, 647, 639, 581, 575 cm^{-1} . MS, m/z (%): 506.9 (100, M + Na). HRMS, (ESI+) for ($\text{C}_{33}\text{H}_{18}\text{Cl}_2 + \text{Na}^+$): calcd 507.06778, found 507.06766. Anal. calcd for $\text{C}_{33}\text{H}_{18}\text{Cl}_2$: C, 81.65; H, 3.74. Found: C, 81.71; H, 3.56.

9-[2,3-Dichloro-4-methyl(d_3)phenylbuta-1,3-diyne]-10-ethynyltriptycene (36). According to GP 2, 36 was synthesized from 32 (320 mg, 0.571 mmol) and a mixture of TBAF in THF (1.0 M, 685 μL , 0.685 mmol) with THF (8 mL). Column chromatography on silica gel (hexane/ CH_2Cl_2 , 3:1) gave 36 as a white crystalline solid (274 mg, 0.561 mmol, 98%).

Mp 300.2–301.3 °C. ¹H NMR (400 MHz, $\text{THF}-d_6$): δ 3.96 (s, 1H), 7.09–7.14 (m, 6H), 7.31 (d, J = 7.95 Hz, 1H), 7.62 (d, J = 7.94 Hz, 1H), 7.72–7.74 (m, 3H), 7.75–7.77 (m, 3H). ²H NMR (76 MHz, $\text{THF}-d_6$): δ 2.45 (s, 3D). ¹³C NMR (100 MHz, $\text{THF}-d_6$): δ 53.3, 54.2, 75.6, 77.5, 78.4, 78.7, 80.1, 83.3, 121.9, 122.8, 123.2, 126.8, 126.9, 130.1, 133.2, 134.3, 136.2, 141.4, 144.0, 144.1 (Carbon signal of CD_3 was not detected due to strong ¹³C–²H coupling). IR (KBr): 3294, 3282, 3094, 3069, 3046, 3032, 3016, 3006, 2956, 2854, 2248, 2233, 2220, 2161, 2057, 1607, 1581, 1454, 1445, 1371, 1342, 1305, 1295, 1259, 1238, 1216, 1164, 1157, 1098, 1068, 1056, 1040, 1033, 978, 954, 950, 924, 878, 869, 800, 765, 752, 747, 699, 676, 657, 653, 647, 639, 573, 568, 507, 492, 478 cm^{-1} . MS, m/z (%): 488.1 (100, M + H). HRMS, (APCI) for ($\text{C}_{33}^1\text{H}_{15}^2\text{H}_3\text{Cl}_2 + \text{H}^+$): calcd 488.10466, found 488.10458. Anal. calcd for $\text{C}_{33}^1\text{H}_{15}^2\text{H}_3\text{Cl}_2$ + THF in 3:1 ratio: C, 80.47; H, 4.09. Found: C, 80.46; H, 3.90.

9-((6-Methylpyridazin-3-yl)buta-1,3-diyne)-10-ethynyltriptycene (37). According to GP 2, 37 was synthesized from 33 (220 mg, 0.448 mmol) and a mixture of TBAF in THF (1.0 M, 538 μL , 0.538 mmol) with THF (10 mL). Column chromatography on silica gel (hexane/acetone, 1:1) gave 37 as a white crystalline solid (182 mg, 0.435 mmol, 97%).

Mp > 230 °C (dec.). ¹H NMR (400 MHz, $\text{THF}-d_6$): δ 2.72 (s, 3H), 3.98 (s, 1H), 7.10–7.15 (m, 6H), 7.49 (d, J = 8.60 Hz, 1H), 7.72–7.77 (m, 6H), 7.77 (d, J = 8.64 Hz, 1H). ¹³C NMR (100 MHz, $\text{THF}-d_6$): δ 22.5, 53.3, 54.1, 76.1, 76.6, 77.2, 78.4, 80.1, 83.4, 122.8, 123.2, 126.5, 126.87, 126.94, 131.0, 143.9, 144.1, 145.7, 159.9. IR (KBr): 3308, 3281, 3070, 3049, 3036, 3018, 2919, 2246, 2162, 1607, 1578, 1539, 1454, 1445, 1410, 1345, 1314, 1304, 1292, 1275, 1245, 1231, 1212, 1174, 1153, 1115, 1080, 1039, 1033, 946, 923, 877, 850, 819, 811, 768, 754, 660, 651, 638, 600 cm^{-1} . MS, m/z (%): 441.2 (100, M + Na), 419.2 (45, M + H). HRMS, (ESI+) for ($\text{C}_{31}\text{H}_{18}\text{N}_2 + \text{H}^+$): calcd 419.15428, found 419.15422. Anal. calcd for $\text{C}_{31}\text{H}_{18}\text{N}_2$: C, 88.97; H, 4.34; N, 6.69. Found: C, 88.84; H, 4.24; N, 6.47.

Compound 38. A solution of *n*-BuLi in hexane (1.6 M, 697 μL , 1.115 mmol) was added dropwise to a stirred solution of alkyne 34 (210 mg, 0.446 mmol) in THF (20 mL) at –78 °C. The yellowish orange solution was stirred at –78 °C for 30 min. Gaseous CO_2 was bubbled into the solution through a PTFE cannula at –78 °C for 10 min and at room temperature for additional 10 min. A dense white

solid precipitated. The white suspension was dissolved upon addition of water (30 mL), and the aqueous phase was washed with CH_2Cl_2 (2×30 mL) and ether (2×20 mL). Acidification of the clear aqueous phase with concentrated HCl (pH ≈ 1) causes immediate precipitation of a dense white solid, which was filtered on a frit, washed with water (3×15 mL), hexane (3×15 mL), CH_2Cl_2 (1×10 mL), and ether (1×10 mL) and dried using Kugelrohr distillation apparatus (60 min, 100 °C, 500 mTorr). The dicarboxylic acid **38** was obtained as a white crystalline solid (222 mg, 0.397 mmol, 89%).

Mp > 250 °C (dec.). ^1H NMR (400 MHz, $\text{THF}-d_6$): δ 7.10–7.12 (m, 6H), 7.68–7.71 (m, 6H), 7.74–7.79 (m, 2H). ^{13}C NMR (100 MHz, $\text{THF}-d_6$): δ 53.1, 54.2, 75.1, 77.3, 80.3, 80.7, 81.1, 86.7, 123.0, 126.4, 127.2, 129.9, 133.1, 133.2, 135.5, 137.6, 143.3, 143.7, 154.2, 165.9. IR (KBr): 3069, 3032, 2978, 2871, 2634, 2544, 2251, 2167, 1700, 1606, 1582, 1529, 1486, 1454, 1443, 1403, 1364, 1308, 1286, 1277, 1241, 1176, 1158, 1141, 1124, 1097, 1066, 1046, 1032, 982, 951, 911, 878, 845, 778, 759, 751, 731, 705, 676, 639, 626, 612, 591, 570, 554 cm^{-1} . MS, m/z (%): 557.2 (52, M), 513.2 (100, M – COOH), 469.2 (41, M – $2 \times \text{COOH}$), 433.2 (30). HRMS, (ESI $^-$) for ($\text{C}_{34}\text{H}_{15}\text{Cl}_2\text{O}_4$): calcd 557.03529, found 557.03513. Anal. calcd for $\text{C}_{34}\text{H}_{16}\text{Cl}_2\text{O}_4$: C, 73.00; H, 2.88. Found: C, 73.29; H, 2.94.

9-((2,3-Dichloro-4-iodophenyl)buta-1,3-diyne)tritycene (39). A flame-dried Schlenk flask was charged with **19** (250 mg, 0.827 mmol), 1,4-diiodo-2,3-dichlorobenzene (1.649 g, 4.134 mmol, 5 equiv), $\text{Pd}(\text{PPh}_3)_4$ (38 mg, 0.033 mmol, 4 mol %), and CuI (5 mg, 0.025 mmol, 3 mol %). After three successive vacuum/argon cycles, degassed dry THF (20 mL) and triethylamine (10 mL) were added from a syringe. The slightly yellowish solution was stirred for 18 h at room temperature. A dense white solid precipitated. The crude reaction mixture was diluted with ether (100 mL) and washed with saturated aqueous NH_4Cl (2×30 mL). A clear yellowish organic phase was dried over MgSO_4 , and volatiles were removed under reduced pressure. Column chromatography on silica gel (hexane/ CH_2Cl_2 , 5:1) provided **39** as a white crystalline solid (427 mg, 0.745 mmol, 90%).

Mp 308.7–309.6 °C. ^1H NMR (400 MHz, CDCl_3): δ 5.43 (s, 1H), 7.04–7.11 (m, 6H), 7.28 (d, $J = 8.27$ Hz, 1H), 7.40–7.42 (m, 3H), 7.74–7.76 (m, 3H), 7.81 (d, $J = 8.26$ Hz, 1H). ^{13}C NMR (100 MHz, CDCl_3): δ 53.2, 53.8, 73.8, 75.9, 80.1, 80.9, 100.6, 122.4, 123.6, 123.7, 125.3, 125.9, 132.8, 135.2, 137.9, 138.0, 143.7, 144.1. IR (KBr): 3068, 3037, 3013, 3004, 2961, 2247, 1609, 1581, 1559, 1457, 1437, 1414, 1353, 1289, 1263, 1227, 1189, 1171, 1153, 1144, 1133, 1093, 1061, 1026, 974, 942, 912, 869, 862, 831, 823, 815, 794, 788, 751, 742, 694, 641, 608, 573, 559, 530, 524, 488, 476 cm^{-1} . MS, m/z (%): 573.2 (100, M + H). HRMS, (APCI) for ($\text{C}_{30}\text{H}_{15}\text{Cl}_2\text{I} + \text{H}^+$): calcd 572.96683, found 572.96682. Anal. calcd for $\text{C}_{30}\text{H}_{15}\text{Cl}_2\text{I}$: C, 62.86; H, 2.64. Found: C, 62.74; H, 2.62.

9-((4-Bromophenyl)buta-1,3-diyne)tritycene (40). A flame-dried Schlenk flask was charged with **19** (500 mg, 1.654 mmol), 1-bromo-4-iodobenzene (561 mg, 1.985 mmol, 1.2 equiv), $\text{Pd}(\text{PPh}_3)_4$ (76 mg, 0.066 mmol, 4 mol %), and CuI (9 mg, 0.050 mmol, 3 mol %). After three successive vacuum/argon cycles, degassed dry THF (5 mL) and triethylamine (5 mL) were added from a syringe. The slightly yellowish solution was stirred for 18 h at room temperature. A dense white solid precipitated. A crude reaction mixture was diluted with ether (150 mL) and washed with saturated aqueous NH_4Cl (2×40 mL). A clear yellowish organic phase was dried over MgSO_4 , and volatiles were removed under reduced pressure. Column chromatography on silica gel (hexane/ CH_2Cl_2 , 5:1) provided **40** as a white crystalline solid (740 mg, 1.618 mmol, 98%).

Mp 239.7–240.9 °C. ^1H NMR (400 MHz, CDCl_3): δ 5.44 (s, 1H), 7.05–7.11 (m, 6H), 7.40–7.42 (m, 3H), 7.51–7.57 (m, 4H), 7.76–7.78 (m, 3H). ^{13}C NMR (100 MHz, CDCl_3): δ 53.1, 53.8, 74.9, 76.3, 77.1, 78.5, 120.5, 122.4, 123.5, 124.0, 125.3, 125.9, 131.9, 134.0, 143.8, 144.1. IR (KBr): 3070, 3041, 2960, 2238, 2154, 1607, 1486, 1457, 1390, 1334, 1288, 1228, 1186, 1176, 1138, 1083, 1067, 1026, 1008, 960, 941, 865, 826, 821, 752, 746, 693, 641, 607, 525, 485, 465 cm^{-1} . MS, m/z (%): 457.1 (100, M + H). HRMS, (APCI) for ($\text{C}_{30}\text{H}_{17}\text{Br} + \text{H}^+$): calcd 457.05864, found 457.05874. Anal. calcd for $\text{C}_{30}\text{H}_{17}\text{Br}$: C, 78.78; H, 3.75. Found: C, 78.58; H, 3.72.

9-((4-Iodophenyl)buta-1,3-diyne)tritycene (41). A flame-dried Schlenk flask was charged with **40** (310 mg, 0.678 mmol), dry NaI (203 mg, 1.356 mmol, 2 equiv), and CuI (6 mg, 0.034 mmol, 5 mol %). After three successive vacuum/argon cycles, degassed dry 1,4-dioxane (1 mL) and racemic *trans*- N,N' -dimethyl-1,2-cyclohexanediamine (11 μL , 0.068 mmol, 10 mol %) were added. A yellowish suspension was stirred at 110 °C for 24 h, allowed to reach room temperature, diluted with ether (80 mL), and washed with saturated aqueous NH_4Cl (2×40 mL). The clear yellow organic phase was dried over MgSO_4 , and volatiles were removed under reduced pressure. Column chromatography on silica gel (hexane/ CH_2Cl_2 , 5:1) yielded **41** as a white crystalline solid (309 mg, 0.613 mmol, 90%).

Mp 261.2–262.6 °C. ^1H NMR (400 MHz, CDCl_3): δ 5.45 (s, 1H), 7.05–7.12 (m, 6H), 7.37–7.43 (m, 5H), 7.75–7.78 (m, 5H). ^{13}C NMR (100 MHz, CDCl_3): δ 53.1, 53.7, 75.1, 76.3, 77.2, 78.6, 95.8, 121.0, 122.4, 123.5, 125.3, 125.9, 134.0, 137.7, 143.8, 144.1. IR (KBr): 3067, 3036, 3017, 2955, 2178, 2153, 1607, 1482, 1457, 1389, 1334, 1289, 1262, 1220, 1187, 1169, 1143, 1083, 1059, 1026, 1006, 980, 943, 904, 870, 860, 820, 753, 746, 733, 702, 689, 641, 606, 523, 483 cm^{-1} . MS, m/z (%): 505.0 (100, M + H). HRMS, (APCI) for ($\text{C}_{30}\text{H}_{17}\text{I} + \text{H}^+$): calcd 505.04477, found 505.04477. Anal. calcd for $\text{C}_{30}\text{H}_{17}\text{I}$: C, 71.44; H, 3.40. Found: C, 71.28; H, 3.35.

Compound 42. A flame-dried Schlenk flask was charged with **39** (300 mg, 0.523 mmol), **7** (229 mg, 0.576 mmol), $\text{Pd}(\text{PPh}_3)_4$ (24 mg, 0.021 mmol, 4 mol %), and CuI (3 mg, 0.016 mmol, 3 mol %). After three successive vacuum/argon cycles, dry and degassed THF (20 mL) and triethylamine (10 mL) were added from a syringe. The yellow solution was stirred for 18 h at room temperature. A dense white solid precipitated. The crude reaction mixture was diluted with CH_2Cl_2 (100 mL), washed with saturated aqueous NH_4Cl (2×30 mL), and the yellowish organic phase was dried over MgSO_4 . Volatiles were removed under reduced pressure. Column chromatography on silica gel (hexane/ CH_2Cl_2 , 3:1) gave **42** as a white crystalline solid (437 mg, 0.518 mmol, 99%).

Mp > 300 °C (dec.). ^1H NMR (400 MHz, CDCl_3): δ 0.50 (s, 9H), 5.46 (s, 1H), 7.06–7.19 (m, 3H), 7.10–7.12 (m, 3H), 7.13–7.16 (m, 6H), 7.41–7.42 (m, 3H), 7.62 (s, 2H), 7.75–7.78 (m, 9H). ^{13}C NMR (100 MHz, CDCl_3): δ 0.3, 53.0, 53.1, 53.2, 53.8, 73.9, 74.1, 75.9, 76.3, 81.17, 81.18, 81.4, 81.7, 98.4, 99.2, 122.1, 122.4, 122.5, 123.6, 124.3, 124.4, 125.3, 125.9, 125.97, 126.01, 131.9, 136.40, 136.41, 142.8, 143.1, 143.7, 144.1. IR (KBr): 3069, 3035, 3018, 3007, 2958, 2951, 2240, 2178, 1607, 1580, 1454, 1369, 1330, 1297, 1290, 1250, 1230, 1221, 1169, 1153, 1142, 1119, 1104, 1056, 1032, 1028, 983, 946, 857, 843, 829, 777, 754, 749, 697, 660, 639, 617, 607, 584, 551, 542, 526, 493, 478 cm^{-1} . MS, m/z (%): 843.2 (100, M + H), 771.2 (18, M – TMS). HRMS, (APCI) for ($\text{C}_{59}\text{H}_{36}\text{Cl}_2\text{Si} + \text{H}^+$): calcd 843.20361, found 843.20404. Anal. calcd for $\text{C}_{59}\text{H}_{36}\text{Cl}_2\text{Si}$: C, 83.97; H, 4.30. Found: C, 83.75; H, 4.31.

Compound 43. A flame-dried Schlenk flask was charged with **41** (260 mg, 0.516 mmol, 1.0 equiv), **7** (226 mg, 0.567 mmol, 1.1 equiv), $\text{Pd}(\text{PPh}_3)_4$ (24 mg, 0.021 mmol, 4 mol %), and CuI (3 mg, 0.015 mmol, 3 mol %). After three successive vacuum/argon cycles, degassed dry THF (5 mL) and triethylamine (5 mL) were added from a syringe. The slightly yellowish solution was stirred for 18 h at room temperature. A dense white solid precipitated. The crude reaction mixture was diluted with CH_2Cl_2 (150 mL) and washed with saturated aqueous NH_4Cl (2×30 mL). The clear yellowish organic phase was dried over MgSO_4 , and volatiles were removed under reduced pressure. Column chromatography on silica gel (hexane/ CH_2Cl_2 , 4:1) gave **43** as a white crystalline solid (377 mg, 0.486 mmol, 94%).

Mp > 320 °C (dec.). ^1H NMR (400 MHz, CDCl_3): δ 0.51 (s, 9H), 5.46 (s, 1H), 7.07–7.14 (m, 6H), 7.14–7.18 (m, 6H), 7.43–7.44 (m, 3H), 7.70 (s, 4H), 7.77–7.81 (m, 9H). ^{13}C NMR (100 MHz, CDCl_3): δ 0.3, 52.95, 53.03, 53.1, 53.8, 76.2, 76.3, 76.4, 76.6, 77.5, 77.7, 78.8, 79.3, 98.3, 99.2, 122.1, 122.38, 122.41, 122.6, 123.5, 125.3, 125.8, 125.89, 125.93, 132.8, 142.9, 143.0, 143.8, 144.1. IR (KBr): 3069, 3046, 3016, 2959, 2895, 2239, 2182, 2155, 1607, 1507, 1497, 1457, 1403, 1334, 1294, 1289, 1251, 1231, 1213, 1188, 1170, 1155, 1139, 1102, 1055, 1032, 1026, 1015, 908, 859, 837, 747, 640, 613, 607, 568, 545, 526, 484, 476, 458 cm^{-1} . MS, m/z (%): 775.3 (100, M + H).

HRMS, (APCI) for (C₅₉H₃₈Si + H⁺): calcd 775.28155, found 775.28168. Anal. calcd for C₅₉H₃₈Si: C, 91.43; H, 4.94. Found: C, 91.20; H, 4.89.

Compound 44. According to GP 2, 44 was synthesized from 42 (350 mg, 0.415 mmol) and a solution of TBAF in THF (1.0 M, 500 μL, 0.500 mmol) in THF (15 mL). Column chromatography on silica gel (hexane/CH₂Cl₂, 3:1) gave 44 as a white crystalline solid (315 mg, 0.408 mmol, 98%).

Mp > 340 °C (dec.). ¹H NMR (500 MHz, THF-*d*₆): δ 4.00 (s, 1H), 5.56 (s, 1H), 7.03–7.08 (m, 6H), 7.11–7.16 (m, 6H), 7.42–7.43 (m, 3H), 7.68–7.70 (m, 3H), 7.72–7.74 (m, 3H), 7.76–7.78 (m, 3H), 7.82 (s, 2H). ¹³C NMR (125 MHz, THF-*d*₆): δ 53.3, 53.9, 54.2, 54.9, 74.8, 75.1, 76.7, 77.2, 78.3, 81.6, 81.9, 82.1, 82.9, 83.5, 122.8, 123.3, 124.6, 125.2, 125.5, 126.1, 126.86, 126.88, 127.0, 133.6, 136.9, 143.9, 144.1, 144.8, 145.6. IR (KBr): 3305, 3068, 3035, 3015, 2951, 2923, 2867, 2854, 2240, 1607, 1580, 1454, 1368, 1329, 1290, 1228, 1243, 1218, 1190, 1156, 1142, 1033, 1026, 978, 946, 910, 860, 829, 811, 751, 735, 654, 647, 639, 607, 553, 486, 479 cm⁻¹. MS, *m/z* (%): 771.2 (100, M + H). HRMS, (APCI) for (C₅₆H₂₈Cl₂ + H⁺): calcd 771.16408, found 771.16384. Anal. calcd for C₅₆H₂₈Cl₂: C, 87.16; H, 3.66. Found: C, 87.09; H, 3.65.

Compound 45. According to GP 2, 45 was synthesized from 43 (500 mg, 0.645 mmol) and a solution of TBAF in THF (1.0 M, 770 μL, 0.770 mmol) in THF (10 mL). Column chromatography on silica gel (hexane/CH₂Cl₂, 2:1) gave 45 as a white crystalline solid (424 mg, 0.603 mmol, 93%).

Mp > 320 °C (dec.). ¹H NMR (400 MHz, THF-*d*₆): δ 4.00 (s, 1H), 5.56 (s, 1H), 7.02–7.09 (m, 6H), 7.11–7.16 (m, 6H), 7.42–7.44 (m, 3H), 7.70–7.71 (m, 3H), 7.73–7.77 (m, 6H), 7.78 (s, 4H). ¹³C NMR (100 MHz, THF-*d*₆): δ 53.3, 53.9, 54.1, 54.8, 76.5, 76.8, 77.2, 77.7, 78.4, 78.5, 78.8, 79.7, 80.5, 83.5, 122.8, 123.2, 123.4, 123.7, 124.5, 126.1, 126.79, 126.84, 126.9, 133.9, 144.06, 144.11, 145.0, 145.6. IR (KBr): 3294, 3067, 3034, 3016, 2954, 2237, 1608, 1581, 1509, 1498, 1457, 1404, 1331, 1289, 1210, 1187, 1170, 1154, 1140, 1102, 1040, 1032, 1026, 943, 923, 913, 875, 860, 838, 748, 712, 674, 648, 639, 607, 579, 545, 527, 486, 475 cm⁻¹. MS, *m/z* (%): 703.2 (100, M + H). HRMS, (APCI) for (C₅₆H₃₀ + H⁺): calcd 703.24203, found 703.24214. Anal. calcd for C₅₆H₃₀: C, 95.70; H, 4.30. Found: C, 95.62; H, 4.22.

Compound 46. A solution of LiHMDS in THF (1.0 M, 584 μL, 0.584 mmol) was added dropwise to a stirred solution of 44 (300 mg, 0.389 mmol) in THF (30 mL) at –78 °C. The reaction mixture turned yellow immediately. It was stirred for 60 min at –78 °C, ClCOOCH₃ (60 μL, 0.778 mmol) was added, and the resulting suspension was stirred for 30 min at –78 °C. Cooling was discontinued, the reaction mixture was slowly warmed to room temperature and stirred for 60 min. Its color turned from a deep to a bright yellow. It was diluted with ether (150 mL) washed with 5% aqueous HCl (2 × 25 mL), 30% aqueous NaHCO₃ (2 × 25 mL), saturated aqueous NH₄Cl (2 × 25 mL), and the clear yellowish organic phase was dried over MgSO₄. Volatiles were removed under reduced pressure. Column chromatography on silica gel (hexane/CH₂Cl₂, 1:1, then hexane/CH₂Cl₂, 1:3) gave the ester 46 as a white crystalline solid (291 mg, 0.351 mmol, 90%).

Mp > 320 °C (dec.). ¹H NMR (500 MHz, THF-*d*₆): δ 3.94 (s, 3H), 5.56 (s, 1H), 7.02–7.09 (m, 6H), 7.15–7.19 (m, 6H), 7.42–7.43 (m, 3H), 7.68–7.70 (m, 3H), 7.71–7.73 (m, 3H), 7.75–7.77 (m, 3H), 7.82 (s, 2H). ¹³C NMR (125 MHz, THF-*d*₆): δ 53.1, 53.4, 54.0, 54.3, 54.9, 74.8, 75.3, 76.7, 77.4, 81.3, 81.5, 81.6, 82.0, 83.0, 85.7, 122.8, 123.0, 123.1, 124.6, 125.2, 125.5, 126.1, 126.9, 127.26, 127.29, 133.6, 136.9, 143.1, 143.7, 144.8, 145.6, 154.0. IR (KBr): 3069, 3048, 3036, 3017, 2957, 2925, 2852, 2249, 2163, 1723, 1607, 1495, 1454, 1434, 1370, 1339, 1330, 1307, 1290, 1272, 1235, 1216, 1189, 1153, 1144, 1128, 1106, 1068, 1033, 1027, 986, 946, 859, 829, 749, 639, 606, 550, 481 cm⁻¹. MS, *m/z* (%): 829.2 (100, M + H). HRMS, (APCI) for (C₅₈H₃₀Cl₂O₂ + H⁺): calcd 829.16956, found 829.16989. Anal. calcd for C₅₈H₃₀Cl₂O₂: C, 83.95; H, 3.64. Found: C, 83.74; H, 3.60.

Compound 47. A solution of LiHMDS in THF (1.0 M, 812 μL, 0.812 mmol) was added dropwise to a stirred solution of 45 (380 mg, 0.541 mmol) in THF (30 mL) at –78 °C. The reaction mixture

turned yellow immediately, was stirred for 60 min at –78 °C, ClCOOCH₃ (84 μL, 1.082 mmol) was added, and the clear yellowish solution was stirred for 30 min at –78 °C. Cooling was discontinued, the reaction mixture was slowly warmed to room temperature and stirred for additional 60 min. The reaction mixture was diluted with ether (150 mL), washed with 5% aqueous HCl (2 × 25 mL), 30% aqueous NaHCO₃ (2 × 25 mL), and saturated aqueous NH₄Cl (2 × 25 mL), and the clear yellowish organic phase was dried over MgSO₄. Volatiles were removed under reduced pressure. Column chromatography on silica gel (hexane/CH₂Cl₂, 1:1, then hexane/CH₂Cl₂, 1:2) gave the ester 47 as a white crystalline solid (371 mg, 0.488 mmol, 90%).

Mp > 310 °C (dec.). ¹H NMR (400 MHz, THF-*d*₆): δ 3.95 (s, 3H), 5.56 (s, 1H), 7.02–7.09 (m, 6H), 7.14–7.19 (m, 6H), 7.42–7.43 (m, 3H), 7.69–7.73 (m, 6H), 7.76–7.78 (m, 7H). ¹³C NMR (100 MHz, THF-*d*₆): δ 53.0, 53.4, 53.9, 54.2, 54.8, 76.4, 76.8, 77.2, 77.9, 78.4, 79.0, 79.2, 80.5, 81.3, 85.7, 122.8, 122.9, 123.2, 123.3, 123.8, 124.5, 126.1, 126.8, 127.2, 127.3, 133.9, 143.1, 143.8, 145.0, 145.6, 154.0. IR (KBr): 3068, 3035, 3017, 2954, 2247, 1723, 1607, 1582, 1508, 1454, 1434, 1404, 1338, 1306, 1269, 1230, 1210, 1188, 1178, 1141, 1110, 1066, 1032, 1026, 979, 942, 860, 838, 823, 747, 694, 639, 607, 542, 526, 486 cm⁻¹. MS, *m/z* (%): 761.2 (100, M + H). HRMS, (APCI) for (C₅₈H₃₂O₂ + H⁺): calcd 761.24751, found 761.24744. Anal. calcd for C₅₈H₃₂O₂: C, 91.56; H, 4.24. Found: C, 91.48; H, 4.22.

Compound 48. According to GP 1, 48 was obtained as a major side product during Sonogashira coupling of 7 (575 mg, 1.443 mmol) with 40 (600 mg, 1.312 mmol). The reaction was done at 80 °C. Column chromatography on silica gel (hexane/CH₂Cl₂, 3:1) provided 48 as a white crystalline solid (133 mg, 0.167 mmol, 23%).

Mp > 250 °C (dec.). ¹H NMR (400 MHz, CDCl₃): δ 0.50 (s, 18H), 7.15–7.17 (m, 12H), 7.73–7.77 (m, 12H). ¹³C NMR (100 MHz, CDCl₃): δ 0.3, 52.86, 52.92, 62.0, 63.9, 74.2, 76.8, 98.4, 99.0, 122.0, 122.5, 125.9, 126.1, 142.6, 142.9. IR (KBr): 3069, 3035, 3017, 2958, 2897, 2227, 2174, 1606, 1580, 1454, 1444, 1409, 1307, 1250, 1232, 1162, 1155, 1141, 1122, 1056, 1033, 1010, 978, 908, 844, 758, 751, 737, 697, 659, 650, 639, 609, 494, 487, 471 cm⁻¹. MS, *m/z* (%): 795.3 (100, M + H). HRMS, (APCI) for (C₅₈H₄₂Si₂ + H⁺): calcd 795.28978, found 795.28979. Anal. calcd for C₅₈H₄₂Si₂ + CDCl₃ in 3:1 ratio: C, 83.88; H, 5.15. Found: C, 83.82; H, 5.11.

■ ASSOCIATED CONTENT

📄 Supporting Information

The Supporting Information is available free of charge on the ACS Publications website at DOI: 10.1021/acs.joc.5b01753.

Copies of ¹H, ¹³C NMR spectra of all new compounds, ¹H and ¹³C NMR assignments in 2, 3, 4, 5, 19, 38, 44, and a packing view of crystals of 4, 6, 18, 19, 20, 22, 39, 40, and 48 (PDF)

Crystallographic data 4 (CIF)

Crystallographic data 6 (CIF)

Crystallographic data 18 (CIF)

Crystallographic data 19 (CIF)

Crystallographic data 20 (CIF)

Crystallographic data 22 (CIF)

Crystallographic data 39 (CIF)

Crystallographic data 40 (CIF)

Crystallographic data 48 (CIF)

■ AUTHOR INFORMATION

Corresponding Author

*kaleta@uochb.cas.cz

Notes

The authors declare no competing financial interest.

ACKNOWLEDGMENTS

This work was supported by the European Research Council under the European Community's Framework Programme (FP7/2007-2013) ERC grant agreement no. 227756, by the Institute of Organic Chemistry and Biochemistry, Academy of Sciences of the Czech Republic (RVO: 61388963) and by the National Science Foundation under grant no. CHE 1265922. The Advanced Light Source is supported by the Director, Office of Science, Office of Basic Energy Sciences, of the U.S. Department of Energy under contract no. DE-AC02-05CH11231. We are grateful to Dr. Lucie Bednářová for help with IR spectra, Dr. Radek Pohl for help with NMR spectra and Dr. Jakub Chalupský for help with visualization of calculated transition moments.

REFERENCES

- (1) *Molecular Motors*; Schliwa, M., Ed.; Wiley-VCH: Weinheim, 2003.
- (2) Kottas, G. S.; Clarke, L. I.; Horinek, D.; Michl, J. *Chem. Rev.* **2005**, *105*, 1281.
- (3) Lemouchi, C.; Iliopoulos, K.; Zorina, L.; Simonov, S.; Wzietek, P.; Cauchy, T.; Fortea, A.; Canadell, E.; Kaleta, J.; Michl, J.; Gindre, D.; Chrysos, M.; Batail, P. *J. Am. Chem. Soc.* **2013**, *135*, 9366.
- (4) Michl, J.; Sykes, E. C. H. *ACS Nano* **2009**, *3*, 1042.
- (5) Horansky, R. D.; Magnera, T. F.; Price, J. C.; Michl, J. *Lect. Notes Phys.* **2007**, *711*, 303.
- (6) Lemouchi, C.; Yamamoto, H. M.; Kato, R.; Simonov, S.; Zorina, L.; Rodriguez-Fortea, A.; Canadell, E.; Wzietek, P.; Iliopoulos, K.; Gindre, D.; Chrysos, M.; Batail, P. *Cryst. Growth Des.* **2014**, *14*, 3375.
- (7) Kobr, L.; Zhao, K.; Shen, Y.; Shoemaker, R. K.; Rogers, C. T.; Michl, J. *Cryst. Growth Des.* **2014**, *14*, 559.
- (8) Kobr, L.; Zhao, K.; Shen, Y.; Comotti, A.; Bracco, S.; Shoemaker, R. K.; Sozzani, P.; Clark, N. A.; Price, J. C.; Rogers, C. T.; Michl, J. *J. Am. Chem. Soc.* **2012**, *134*, 10122.
- (9) Zhao, K.; Dron, P. I.; Kaleta, J.; Rogers, C. T.; Michl, J. *Top. Curr. Chem.* **2014**, *354*, 163.
- (10) Kaleta, J.; Michl, J.; Mazal, C. *J. Org. Chem.* **2010**, *75*, 2350.
- (11) *Molecular Machines and Motors*; Credi, A., Silvi, S., Venturi, M., Eds.; Springer: Heidelberg, 2014.
- (12) Bastien, G.; Lemouchi, C.; Allain, M.; Wzietek, P.; Rodriguez-Fortea, A.; Canadell, E.; Iliopoulos, K.; Gindre, D.; Chrysos, M.; Batail, P. *CrystEngComm* **2014**, *16*, 1241.
- (13) Perez-Estrada, S.; Rodriguez-Molina, B.; Xiao, L.; Santillan, R.; Jimenez-Oses, G.; Houk, K. N.; Garcia-Garibay, M. A. *J. Am. Chem. Soc.* **2015**, *137*, 2175.
- (14) Acros-Ramos, R.; Rodriguez-Molina, B.; Gonzales-Rodriguez, E.; Ramirez-Montes, P. I.; Ochoa, M. E.; Santillan, R.; Farfan, N.; Garcia-Gariba, M. A. *RSC Adv.* **2015**, *5*, 55201.
- (15) Rozenbaum, V. M.; Ogenko, V. M.; Chuiko, A. A. *Sov. Phys. Usp.* **1991**, *34*, 883.
- (16) Cipolloni, M.; Kaleta, J.; Mašát, M.; Dron, P. I.; Shen, Y.; Zhao, K.; Rogers, C. T.; Shoemaker, R. K.; Michl, J. *J. Phys. Chem. C* **2015**, *119*, 8805.
- (17) Kaleta, J.; Dron, P. I.; Zhao, K.; Shen, Y.; Císařová, I.; Rogers, C. T.; Michl, J. *J. Org. Chem.* **2015**, *80*, 6173.
- (18) Iimura, K.; Kato, T. *Langmuir-Blodgett (LB) Film*. In *Organized Organic Ultrathin Films, Fundamentals and Applications*; Ariga, K., Ed.; Wiley-VCH Verlag GmbH & Co. KGaA: Weinheim, Germany, 2013; p 43.
- (19) Bune, A.; Ducharme, S.; Fridkin, V.; Blinov, L.; Palto, S.; Petukhova, N.; Yudin, S. *Appl. Phys. Lett.* **1995**, *67*, 3975.
- (20) Ducharme, S.; Reece, T. J.; Othon, C. M.; Rannow, R. K. *IEEE Trans. Device Mater. Reliab.* **2005**, *5*, 720.
- (21) Batirov, T. M.; Ducharme, S.; Fridkin, V. M.; Kuznetsova, N.; Palto, S. P.; Verkhovskaya, K. A.; Vizdrik, G.; Yudin, S. G. *Integr. Ferroelectr.* **2001**, *37*, 155.
- (22) Ducharme, S.; Bune, A.; Fridkin, V.; Blinov, L.; Palto, S.; Petukhova, N.; Yudin, S. *Ferroelectrics* **1997**, *202*, 29.
- (23) Bune, A. V.; Fridkin, V. M.; Ducharme, S.; Blinov, L. M.; Palto, S. P.; Sorokin, A. V.; Yudin, S. G.; Zlatkin, A. *Nature* **1998**, *391*, 874.
- (24) Gerber, A.; Fitsilis, M.; Waser, R.; Reece, T. J.; Rije, E.; Ducharme, S.; Kohlstedt, H. *J. Appl. Phys.* **2010**, *107*, 124119.
- (25) Chong, J.; MacLachlan, M. J. *J. Org. Chem.* **2007**, *72*, 8683.
- (26) Betz, R.; McClelland, C.; Scheffer, A. *Acta Crystallogr., Sect. E: Struct. Rep. Online* **2011**, *67*, o2368.
- (27) Kissel, P.; Murray, D. J.; Wulfstange, W. J.; Catalano, V. J.; King, B. T. *Nat. Chem.* **2014**, *6*, 751.
- (28) Hurdis, E. C.; Smyth, C. P. *J. Am. Chem. Soc.* **1942**, *64*, 2212.
- (29) Li, H.; Franks, K. J.; Hanson, R. J.; Kong, W. *J. Phys. Chem. A* **1998**, *102*, 8084.
- (30) Kobayashi, E.; Jiang, J.; Ohta, H.; Furukawa, J. *J. Polym. Sci., Part A: Polym. Chem.* **1990**, *28*, 2641.
- (31) Caskey, D. C.; Wang, B.; Zheng, X.; Michl, J. *Collect. Czech. Chem. Commun.* **2005**, *70*, 1970.
- (32) Keller, S.; Yi, Ch.; Li, Ch.; Liu, S.-X.; Blum, C.; Frei, G.; Sereda, O.; Neels, A.; Wandlowski, T.; Decurtins, S. *Org. Biomol. Chem.* **2011**, *9*, 6410.
- (33) Toyota, S.; Yamamori, T.; Asakura, M.; Oki, M. *Bull. Chem. Soc. Jpn.* **2000**, *73*, 205.
- (34) Kelly, T. R.; Sestelo, J. P.; Tellitu, I. *J. Org. Chem.* **1998**, *63*, 3655.
- (35) Glaxo Group Ltd. Compounds. Patent EP2080761 A1, July 22, 2009.
- (36) Shen, H.; Vollhardt, K. P. C. *Synlett* **2012**, *23*, 208.
- (37) Godinez, C. E.; Zepeda, G.; Garcia-Garibay, M. A. *J. Am. Chem. Soc.* **2002**, *124*, 4701.
- (38) Karlen, S. D.; Godinez, C.; Garcia-Garibay, M. A. *Org. Lett.* **2006**, *8*, 3417.
- (39) Buffeteau, T.; Desbat, B.; Turlet, J. M. *Appl. Spectrosc.* **1991**, *45*, 380.
- (40) Kaleta, J.; Mazal, C. *Org. Lett.* **2011**, *13*, 1326.
- (41) Kaleta, J.; Nečas, M.; Mazal, C. *Eur. J. Org. Chem.* **2012**, *25*, 4783.
- (42) Wilson, E. B. *Phys. Rev.* **1934**, *46*, 146.
- (43) Thiel, P. A. *Surf. Sci. Rep.* **1987**, *7*, 211.
- (44) Debe, M. K. *J. Appl. Phys.* **1984**, *55*, 3354.
- (45) Michl, J.; Thulstrup, E. W. *Spectroscopy with Polarized Light: Solute Alignment by Photoselection, Liquid Crystals, Polymers, and Membranes*, revised soft-cover ed.; VCH Publishers: Deerfield Beach, FL, 1995.
- (46) Arnold, R.; Terfort, A.; Wöll, C. *Langmuir* **2001**, *17*, 4980.
- (47) Chalifoux, W. A.; McDonald, R.; Ferguson, M. J.; Tykwinski, R. *Angew. Chem., Int. Ed.* **2009**, *48*, 7915.
- (48) CambridgeSoft, 1986–2007; www.cambridgesoft.com.
- (49) Frisch, M. J.; Trucks, G. W.; Schlegel, H. B.; Scuseria, G. E.; Robb, M. A.; Cheeseman, J. R.; Scalmani, G.; Barone, V.; Mennucci, B.; Petersson, G. A.; Nakatsuji, H.; Caricato, M.; Li, X.; Hratchian, H. P.; Izmaylov, A. F.; Bloino, J.; Zheng, G.; Sonnenberg, J. L.; Hada, M.; Ehara, M.; Toyota, K.; Fukuda, R.; Hasegawa, J.; Ishida, M.; Nakajima, T.; Honda, Y.; Kitao, O.; Nakai, H.; Vreven, T.; Montgomery, J. A., Jr.; Peralta, J. E.; Ogliaro, F.; Bearpark, M.; Heyd, J. J.; Brothers, E.; Kudin, K. N.; Staroverov, V. N.; Kobayashi, R.; Normand, J.; Raghavachari, K.; Rendell, A.; Burant, J. C.; Iyengar, S. S.; Tomasi, J.; Cossi, M.; Rega, N.; Millam, J. M.; Klene, M.; Knox, J. E.; Cross, J. B.; Bakken, V.; Adamo, C.; Jaramillo, J.; Gomperts, R.; Stratmann, R. E.; Yazyev, O.; Austin, A. J.; Cammi, R.; Pomelli, C.; Ochterski, J. W.; Martin, R. L.; Morokuma, K.; Zakrzewski, V. G.; Voth, G. A.; Salvador, P.; Dannenberg, J. J.; Dapprich, S.; Daniels, A. D.; Farkas, O.; Foresman, J. B.; Ortiz, J. V.; Cioslowski, J.; Fox, D. J. *Gaussian 09, Revision A.02*; Gaussian, Inc.: Wallingford CT, 2009.
- (50) Sheldrick, G. M. *Acta Crystallogr., Sect. A: Found. Crystallogr.* **2008**, *64*, 112.
- (51) Landscheidt, H.; Broda, W.; Klausener, A., Bayer Aktiengesellschaft, Patent US5648570 A, July 15, 1997.
- (52) Marvel, C. S.; Overberger, C. G.; Allen, R. E.; Johnston, H. W.; Saunders, J. H.; Young, J. D. *J. Am. Chem. Soc.* **1946**, *68*, 861.